

The Effect of Fractional-Order Derivative for Pattern Formation of Brusselator Reaction–Diffusion Model Occurring in Chemical Reactions

Mostafa Abbaszadeh^{1*}, Alireza Bagheri Salec² and Shurooq Kamel Abd Al-Khafaji²

¹Department of Applied Mathematics, Faculty of Mathematics and Computer Sciences, Amirkabir University of Technology (Tehran Polytechnic), No. 424, Hafez Ave., 15914 Tehran, Iran

²Department of Mathematics, Faculty of Basic Science, University of Qom Alghadir Blvd., Qom, Iran

Keywords:

Fractional calculus,
Brusselator model,
Spectral method,
Error estimate

AMS Subject Classification (2020):

76M22; 26A33; 65L60

Article History:

Received: 28 August 2023

Accepted: 21 October 2023

Abstract

The space fractional PDEs (SFPDEs) have attracted a lot of attention. Developing high-order and stable numerical algorithms for them is the main aim of most researchers. This research work presents a fractional spectral collocation method to solve the fractional models with space fractional derivative which is defined based upon the Riesz derivative. First, a second-order difference formulation is used to approximate the time derivative. The stability property and convergence order of the semi-discrete scheme are analyzed. Then, the fractional spectral collocation method based on the fractional Jacobi polynomials is employed to discrete the spatial variable. In the numerical results, the effect of fractional order is studied.

© 2023 University of Kashan Press. All rights reserved.

1 Introduction

Turing systems appear in various biological systems, such as patterns in fish, butterflies, lady bugs, tumor growth, and a synthetic bacterial population [1]. We can mention the Gierer-Meinhardt model for pattern formation of spatial tissue structures in morphogenesis [2], the morphodynamic (limit) model in describing the cell dynamics and the chemical processes during limb bud formation [3] and the FitzHugh-Nagumo model for analyzing various processes in the myocardium [4, 5]. Non-monotonic behavior of the critical magnetic Prandtl number is explained in [6] based on an analysis of the intermittency in the convective attractors.

*Corresponding author

E-mail addresses: m.abbaszadeh@aut.ac.ir (M. Abbaszadeh), r-bagheri@qom.ac.ir (A. R. Bagheri Salec), shurooqkamel7@gmail.com (S. K. Abd Al-Khafaji)

Academic Editor: Abbas Saadatmandi

1.1 Governing model

In the current work the space-fractional Brusselator model is considered

$$\frac{\partial u}{\partial t} - \mu_{11} \left(\frac{\partial^{2\nu} u(x, y, t)}{\partial |x|^{2\nu}} + \frac{\partial^{2\nu} u(x, y, t)}{\partial |y|^{2\nu}} \right) = f(u, v), \quad (x, y, t) \in \Omega \times [0, T], \quad (1)$$

$$\frac{\partial v}{\partial t} - \mu_{21} \left(\frac{\partial^{2\eta} u(x, y, t)}{\partial |x|^{2\eta}} + \frac{\partial^{2\eta} u(x, y, t)}{\partial |y|^{2\eta}} \right) = g(u, v), \quad (x, y, t) \in \Omega \times [0, T], \quad (2)$$

where

$$f(u, v) = \gamma_1 (\gamma_2 - u + u^2 v), \quad g(u, v) = \gamma_1 (\gamma_3 - u^2 v), \quad (3)$$

with boundary and initial conditions

$$\frac{\partial u}{\partial \mathbf{n}} = \frac{\partial v}{\partial \mathbf{n}} = 0, \quad (x, y, t) \in \partial\Omega \times [0, T],$$

$$u(x, y, 0) = \psi_1(x, y), \quad v(x, y, 0) = \psi_2(x, y), \quad (x, y) \in \Omega,$$

where Ω is an open and bounded domain, γ_i for $i = 1, 2, 3$ are constants, μ_{ij} for $i, j = 1, 2$ indicate the diffusion coefficients and \mathbf{n} denotes the unit normal vector. Furthermore, in Equations (1) and (2), we consider

$$\frac{\partial^{2\nu} u(x, y, t)}{\partial |x|^{2\nu}} = \frac{-1}{2 \cos(\nu\pi)} \left({}_x^{RL} D_L^{2\nu} u(x, y, t)(x, y, t) + {}_x^{RL} D_R^{2\nu} u(x, y, t)(x, y, t) \right), \quad (4)$$

$$\frac{\partial^{2\eta} u(x, y, t)}{\partial |y|^{2\eta}} = \frac{-1}{2 \cos(\eta\pi)} \left({}_y^{RL} D_L^{2\eta} u(x, y, t)(x, y, t) + {}_y^{RL} D_R^{2\eta} u(x, y, t)(x, y, t) \right), \quad (5)$$

where

$${}_x^{RL} D_L^{2\nu} u(x, y, t) = \frac{1}{\Gamma(2-2\nu)} \frac{\partial^2}{\partial x^2} \int_L^x (x-\xi)^{1-2\nu} u(\xi, y, t) d\xi, \quad (6)$$

$${}_x^{RL} D_R^{2\nu} u(x, y, t) = \frac{1}{\Gamma(2-2\nu)} \frac{\partial^2}{\partial x^2} \int_x^R (\xi-x)^{1-2\nu} u(\xi, y, t) d\xi, \quad (7)$$

$${}_y^{RL} D_L^{2\eta} u(x, y, t) = \frac{1}{\Gamma(2-2\eta)} \frac{\partial^2}{\partial y^2} \int_L^y (y-\xi)^{1-2\eta} u(x, \xi, t) d\xi, \quad (8)$$

$${}_y^{RL} D_R^{2\eta} u(x, y, t) = \frac{1}{\Gamma(2-2\eta)} \frac{\partial^2}{\partial y^2} \int_y^R (\xi-y)^{1-2\eta} u(x, \xi, t) d\xi. \quad (9)$$

and $0 < \nu, \eta \leq 1$.

The integer order of the mathematical model (1) is numerically solved by using different approaches. For example, meshless method [7], finite volume element method [8], finite difference

method [9], variational multiscale element free Galerkin and local discontinuous Galerkin methods [10], modified cubic B-spline differential quadrature method [11], etc. The spatial patterns of a chemical can be produced based on the reaction of chemicals, under specific certain [12, 13] which can be seen in Figure 1. Also, a novel semi-analytical technique i.e. the fractional reduced differential transform method (FRDTM) has been applied in [14] to solve the time-fractional Brusselator reaction-diffusion system which its convergence analysis has been studied here. The main of [15] is to obtain the approximate solution of the fractional nonlinear Brusselator model in the Caputo sense by using the Laplace-Adomian decomposition method (LADM). Authors of [15] established a general scheme for the solution to the Brusselator model by applying the LADM. The time-fractional Brusselator reaction-diffusion model is solved in [16] with the help of the residual power series transform method. The author of [17] investigated the effects of the time-fractional derivative on the oscillations in the fractal-fractional Brusselator chemical reaction (FFBCR). An effective hybrid matrix method is developed in [18] to solve the time-fractional Brusselator reaction-diffusion model based upon the combination of the quasi-linearization technique with the spectral collocation strategy and the generalized clique bases. A dynamical Brusselator reaction-diffusion system arising in the triple collision and enzymatic reactions with time-fractional Caputo derivative is simulated in [19] based on the q -homotopy analysis transform method (q -HATM).

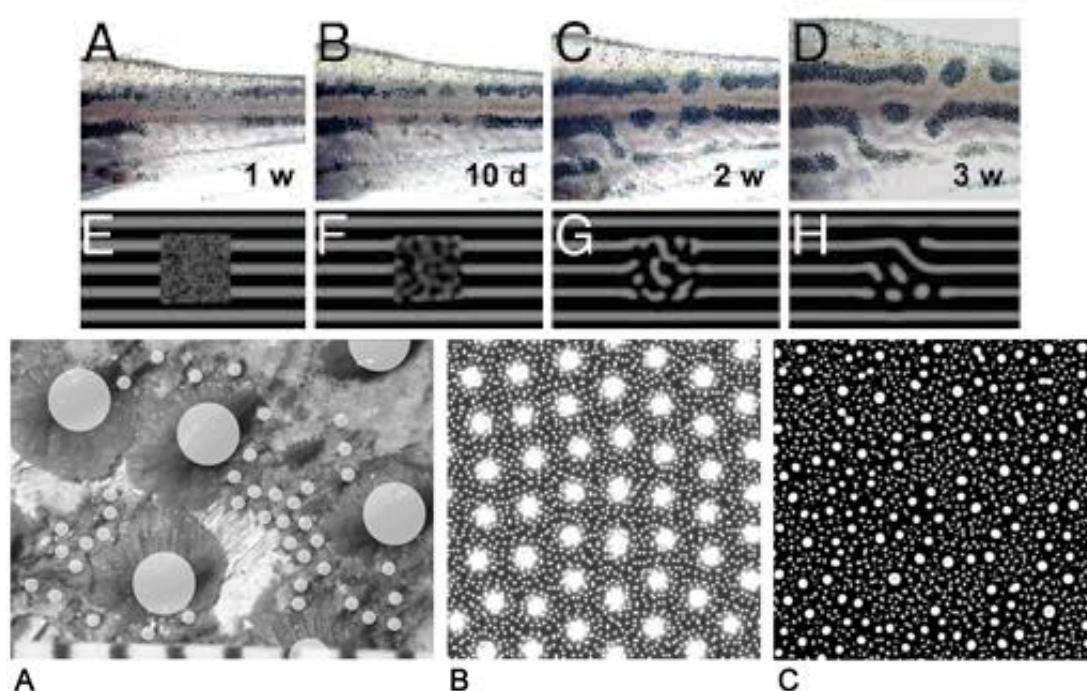


Figure 1: Pattern formation of Brusselator model.

1.2 A brief review of the fractional calculus

In the recent decade, the interest and inclination towards fractional calculations has increased. Because of the varied applications of fractional PDEs and ODEs in the various fields of science

and engineering, including finance [20], chemistry [21], fluid and solid mechanics [22], etc, many researchers have been attracted to this subject. It has been observed that the results of mathematical models with integer-order derivatives are different from outputs of the experimental results [23]. Therefore, many researchers tried to propose analytical and numerical techniques to study fractional PDEs in various cases. The space fractional PDEs with the distributed-order are numerically studied in [24]. On the other hand, the space fractional PDEs are studied in several ways such as a second-order difference formula [25, 26], Legendre operational matrix [27], a tau approach based on the shifted Legendre polynomials [28], a new operational matrix based on Müntz-Legendre polynomials [29], a finite element method [30], the operational matrix of the fractional-order Chebyshev functions [31], the collocation method based on Chebyshev polynomials [32], the sinc functions via Legendre polynomials [33], the high-order difference plans [34–36], the ADI finite difference technique [37], a difference approach with non-uniform grids [38], the spectral formula [39], the fractional spectral collocation discretization for space fractional optimal control problem [40], meshless methods [41], finite difference/spectral method [42], L_1 approximation scheme [43], Logarithmic Jacobi collocation method [44], etc. A fractional order Jacobi Tau method is developed in [45] for the time-fractional PDEs with variable coefficients. A second-order backward difference formula (BDF2) is proposed in [46] for solving time approximation of Riesz space-fractional diffusion equations.

The main aim of [47] is to develop a finite difference scheme for simulating fractional characterization of the MHD fluid model. The simulation of activator–inhibitor dynamics based on a cross-diffusion Brusselator reaction–diffusion system via a differential quadrature–radial point interpolation method (DQ-RPIM) technique is developed in [48]. A reduced-order finite difference method based on the proper orthogonal decomposition is proposed in [49] for solving space-fractional reaction-diffusion systems corresponding to the Gray-Scott model.

2 Some preliminaries

Assume the temporal step size is $\tau = \frac{T}{N}$ and $t_n = n\tau$ for $n = 1, 2, \dots, N$. Next, we approximate the space derivatives and for this aim some definitions are needed.

Definition 2.1. ([50]). The Jacobi polynomials are defined as

$$\begin{cases} P_0^{\varpi_1, \varpi_2}(x) = 1, \\ P_1^{\varpi_1, \varpi_2}(x) = \frac{1}{2}(\varpi_1 + \varpi_2 + 2)x + \frac{1}{2}(\varpi_1 - \varpi_2), \\ P_{n+1}^{\varpi_1, \varpi_2}(x) = (A_n^{\varpi_1, \varpi_2}x - B_n^{\varpi_1, \varpi_2})P_n^{\varpi_1, \varpi_2}(x) - C_n^{\varpi_1, \varpi_2}P_{n-1}^{\varpi_1, \varpi_2}(x), \quad n \geq 1, \end{cases}$$

where

$$\begin{cases} A_n^{\varpi_1, \varpi_2} = \frac{(2n + \varpi_1 + \varpi_2 + 1)(2n + \varpi_1 + \varpi_2 + 2)}{2(n+1)(n + \varpi_1 + \varpi_2 + 1)}, \\ B_n^{\varpi_1, \varpi_2} = \frac{(\varpi_1^2 - \varpi_2^2)(2n + \varpi_1 + \varpi_2 + 1)}{2(n+1)(n + \varpi_1 + \varpi_2 + 1)(2n + \varpi_1 + \varpi_2)}, \\ C_n^{\varpi_1, \varpi_2} = \frac{(n + \varpi_1)(n + \varpi_2)(2n + \varpi_1 + \varpi_2 + 2)}{(n+1)(n + \varpi_1 + \varpi_2 + 1)(2n + \varpi_1 + \varpi_2)}. \end{cases}$$

For $\varpi_1, \varpi_2 > -1$ they are orthogonal with the weight function $\omega^{\varpi_1, \varpi_2} = (1-x)^{\varpi_1}(1+x)^{\varpi_2}$ over interval $(-1, 1)$.

Definition 2.2. ([50]). Let $1 < \alpha < 2$, $0 < \varpi_1, \varpi_2 < \alpha$, $\varpi_1 + \varpi_2 = \alpha$, $0 \leq p \leq 1$ and

$$C(\alpha, \varpi_1, \varpi_2) = \frac{\sin(\pi\varpi_1) + \sin(\pi\varpi_2)}{\sin(\pi\alpha)}. \tag{10}$$

Also, we introduce

$$\mathbb{I}_{0+}^\alpha v(x) = \frac{1}{\Gamma(\alpha)} \int_0^x (x-s)^{\alpha-1} v(s) ds, \quad x > 0,$$

$$\mathbb{I}_{1-}^\alpha v(x) = \frac{1}{\Gamma(\alpha)} \int_x^1 (s-x)^{\alpha-1} v(s) ds, \quad x < 1.$$

We define the following linear operators

$$\mathcal{I}_{-1,1}^{\varpi_1, \varpi_2, \alpha} : = \frac{1}{2} C(\alpha, \varpi_1, \varpi_2) (\mathbb{I}_{0+}^\alpha + \mathbb{I}_{1-}^\alpha), \tag{11}$$

$$\mathcal{D}_{-1,1}^{\varpi_1, \varpi_2, \alpha} : = \frac{d^k}{dx^k} \mathcal{I}_{-1,1}^{\varpi_1, \varpi_2, k-\alpha}, \quad k \in \mathbb{N}, \tag{12}$$

$$\mathcal{J}_m^{-\varrho, -s}(x) = (1-x)^\varrho (1+x)^s P_m^{\varrho, s}, \quad \varrho, s > -1. \tag{13}$$

Lemma 2.3. ([50]). Let $1 < \alpha < 2$ and $0 < \varpi_1, \varpi_2 < \alpha$ with condition $\varpi_1 + \varpi_2 = \alpha$ and

$$\frac{1}{2} \sin(\pi\varpi_1) = \frac{1}{2} \sin(\pi\varpi_2).$$

Then, for $-1 \leq x \leq 1$, $n \in \mathbb{N} \cup \{0\}$ and $k = 1, 2, \dots, n+2$ we have

$$\mathcal{I}_{-1,1}^{\varpi_1, \varpi_2, 2-\alpha} \mathcal{J}_n^{-\varpi_1, -\varpi_2}(x) = \widehat{C}(n, \alpha) P_{n+2}^{\varpi_2-2, \varpi_1-2}, \quad \widehat{C}(n, \alpha) = \frac{4\Gamma(n+\alpha-1)}{n!},$$

$$\mathcal{D}_{-1,1}^{\varpi_1, \varpi_2, k-2+\alpha} \mathcal{J}_n^{-\varpi_1, -\varpi_2}(x) = \widetilde{C}(n, k, \alpha) P_{n+2-k}^{\varpi_2-2+k, \varpi_1-2+k}, \quad \widetilde{C}(n, k, \alpha) = \frac{\Gamma(n+k+\alpha-1)}{2^{k-2} n!}.$$

Let C^0 presents the space of continuous functions.

Definition 2.4. ([51]). Given $\varrho > 0$ then the following semi-norms

$$|v|_{J_L^\varrho(\mathbb{R}^2)} = \left(\| {}^{RL}D_L^\varrho v \|_{L^2(\mathbb{R}^2)}^2 + \| {}^{RL}D_L^\varrho v \|_{L^2(\mathbb{R}^2)}^2 \right)^{\frac{1}{2}}, \tag{14}$$

$$|v|_{J_R^\varrho(\mathbb{R}^2)} = \left(\| {}^{RL}D_R^\varrho v \|_{L^2(\mathbb{R}^2)}^2 + \| {}^{RL}D_R^\varrho v \|_{L^2(\mathbb{R}^2)}^2 \right)^{\frac{1}{2}}, \tag{15}$$

and norms

$$\|v\|_{J_L^\varrho(\mathbb{R}^2)} = \left(\|v\|_{L^2(\mathbb{R}^2)}^2 + |v|_{J_L^\varrho(\mathbb{R}^2)}^2 \right)^{\frac{1}{2}}, \tag{16}$$

$$\|v\|_{J_R^\varrho(\mathbb{R}^2)} = \left(\|v\|_{L^2(\mathbb{R}^2)}^2 + |v|_{J_R^\varrho(\mathbb{R}^2)}^2 \right)^{\frac{1}{2}}. \tag{17}$$

can be defined. Also, $J_L^\varrho(\mathbb{R}^2)$ and $J_R^\varrho(\mathbb{R}^2)$ are the closure of $C_0^\infty(\mathbb{R}^2)$ with respect to $\|v\|_{J_L^\varrho(\mathbb{R}^2)}$ and $\|v\|_{J_R^\varrho(\mathbb{R}^2)}$, respectively.

Definition 2.5. ([51]). Given $\varrho > 0$ then we define the following semi-norm

$$|v|_{H^{\varrho}(\mathbb{R}^2)} = \|\ |\xi|^{\varrho} \widehat{v}(\xi) \|_{L^2(\mathbb{R}^2_{\xi})}, \tag{18}$$

and norm

$$\|v\|_{H^{\varrho}(\mathbb{R}^2)} = \left(\|v\|_{L^2(\mathbb{R}^2)}^2 + |v|_{H^{\varrho}(\mathbb{R}^2)}^2 \right)^{\frac{1}{2}}, \tag{19}$$

where $H^{\varrho}(\mathbb{R}^2)$ is the closure of $C_0^{\infty}(\mathbb{R}^2)$ with respect to $\|v\|_{H^{\varrho}(\mathbb{R}^2)}$ and \widehat{v} is the Fourier transform of v . Furthermore, H_0^{ϱ} denotes the semi-norms.

Definition 2.6. ([51]). Given $\varrho > 0$. If $\varrho \neq n - \frac{1}{2}$ for $n \in \mathbb{N}$ we consider the following semi-norm

$$|v|_{J_S^{\varrho}(\mathbb{R}^2)} = \left(\left| ({}^R L D_x^{\varrho} v, {}^R L D_x^{\varrho} v)_{L^2(\mathbb{R}^2)} \right| + \left| ({}^R L D_y^{\varrho} v, {}^R L D_y^{\varrho} v)_{L^2(\mathbb{R}^2)} \right| \right)^{\frac{1}{2}}, \tag{20}$$

and norm

$$\|v\|_{J_S^{\varrho}(\mathbb{R}^2)} = \left(\|v\|_{L^2(\mathbb{R}^2)}^2 + |v|_{J_S^{\varrho}(\mathbb{R}^2)}^2 \right)^{\frac{1}{2}}. \tag{21}$$

Also, $J_S^{\varrho}(\mathbb{R}^2)$ is the closure of $C_0^{\infty}(\mathbb{R}^2)$ with respect to $\|v\|_{J_S^{\varrho}(\mathbb{R}^2)}$.

Lemma 2.7. ([51]). For $\varrho > 0$ spaces $J_L^{\varrho}(\mathbb{R}^2)$, $J_R^{\varrho}(\mathbb{R}^2)$ and $H^{\varrho}(\mathbb{R}^2)$ are equivalent.

Lemma 2.8. ([51]). Let $v \in J_S^{\varrho}(\Omega)$ and \bar{v} be the deployment of v outside of Ω then

$$({}^R L D_x^{\varrho} v, {}^R L D_b^{\varrho} v)_{L^2(\Omega)} = ({}^R L D_x^{\varrho} \bar{v}, {}^R L D_b^{\varrho} \bar{v})_{L^2(\mathbb{R}^2)} = \cos(\pi\varrho) \|{}^R L D_x^{\varrho} \bar{v}\|_{L^2(\mathbb{R}^2)}^2, \tag{22}$$

$$({}^R L D_y^{\varrho} v, {}^R L D_d^{\varrho} v)_{L^2(\Omega)} = ({}^R L D_y^{\varrho} \bar{v}, {}^R L D_d^{\varrho} \bar{v})_{L^2(\mathbb{R}^2)} = \cos(\pi\varrho) \|{}^R L D_y^{\varrho} \bar{v}\|_{L^2(\mathbb{R}^2)}^2, \tag{23}$$

in which ϱ is the order of fractional.

Lemma 2.9. ([51]). Let $\varrho \in (1, 2)$, $u, v \in J_L^{\varrho}(\Omega)$ where u and v are zero on $\partial\Omega$ then

$$({}^R L D_x^{\varrho} u, v) = \left({}^R L D_x^{\frac{\varrho}{2}} u, {}^R L D_b^{\frac{\varrho}{2}} v \right), \quad ({}^R L D_y^{\varrho} u, v) = \left({}^R L D_y^{\frac{\varrho}{2}} u, {}^R L D_d^{\frac{\varrho}{2}} v \right), \tag{24}$$

$$({}^R L D_b^{\varrho} u, v) = \left({}^R L D_b^{\frac{\varrho}{2}} v, {}^R L D_x^{\frac{\varrho}{2}} v \right), \quad ({}^R L D_d^{\varrho} u, v) = \left({}^R L D_d^{\frac{\varrho}{2}} v, {}^R L D_y^{\frac{\varrho}{2}} v \right). \tag{25}$$

Now, we define the following weighted Sobolev space

$$L_{\omega}^2(\Omega) = \left\{ f : \int_{\Omega} f^2(x)\omega dx < +\infty \right\},$$

with norm

$$\|u\|_{\omega} = \left(\int_{\Omega} f^2(x)\omega dx \right)^{\frac{1}{2}}.$$

For $\omega = 1$, we denote $L^2(\Omega) = L_{\omega}^2(\Omega)$. For $1 < \alpha < 2$, $0 < \varpi_1, \varpi_2 < \alpha$, $l = -1, 0, 1, \dots, m$, $m \in \mathbb{N}$, we denote

$$\mathcal{B}_{\alpha}^m = \left\{ u \in L_{\omega^{-\varpi_1, -\varpi_2}}^2(\Omega) : \mathcal{D}_{-1,1}^{\varpi_1, \varpi_2, \alpha+1} u \in L_{\omega^{\varpi_1+l, \varpi_2+l}}^2(\Omega), \quad -1 \leq l \leq m \right\}.$$

Let \mathbb{P}_N be space of polynomials of degree at most N . Also, we define

$$\mathbb{F}_N^{-\varpi_1, -\varpi_2}(\Omega) = \{u = (1 - x)^{\varpi_1}(1 + x)^{\varpi_2}v : v \in \mathbb{P}_N\}.$$

Define the following $L^2_{\omega^{-\varpi_1, -\varpi_2}}$ -orthogonal projection

$$(\Pi_N^{-\varpi_1, -\varpi_2}u - u, v_N)_{\omega^{-\varpi_1, -\varpi_2}} = 0, \quad \forall v_N \in F_N^{-\varpi_1, -\varpi_2}(\Omega). \tag{26}$$

Thus, we have

$$\Pi_N^{-\varpi_1, -\varpi_2}u(x) = \sum_{n=0}^N \widehat{u}_n^{-\varpi_1, -\varpi_2} \mathcal{J}_n^{-\varpi_1, -\varpi_2}(x), \tag{27}$$

$$\widehat{u}_n^{-\varpi_1, -\varpi_2} = \frac{1}{\gamma_n^{\varpi_1, \varpi_2}} \int_{-1}^1 u(x) \mathcal{J}_n^{-\varpi_1, -\varpi_2}(x) \omega^{-\varpi_1, -\varpi_2}(x) dx,$$

$$\gamma_n^{\varpi_1, \varpi_2} = \frac{2^{\varpi_1 + \varpi_2 + 1} \Gamma(n + \varpi_1 + 1) \Gamma(n + \varpi_2 + 1)}{(2n + \varpi_1 + \varpi_2 + 1) n! \Gamma(n + \varpi_1 + \varpi_2 + 1)}.$$

Theorem 2.10. ([50]). Let $1 < \alpha < 2$ and $u \in \mathcal{B}_\alpha^m$ where $m \in \mathbb{N}$. If $0 < \varpi_1, \varpi_2 < \alpha$ then for $-1 \leq l \leq m \leq N$, $0 \leq m \leq N$ and $C \in \mathbb{R}^+$, we have

$$\|\Pi_N^{-\varpi_1, -\varpi_2}u - u\|_{\omega^{-\varpi_1, -\varpi_2}} \leq CN^{-\alpha - m} \|\mathcal{D}_{-1,1}^{\varpi_1, \varpi_2, \alpha + m}u\|_{\omega^{\varpi_1 + m, \varpi_2 + m}}. \tag{28}$$

3 Time-discrete analysis

We employ a finite difference scheme for the time derivative of the main model as follows:

$$\frac{\partial u^{n-\frac{1}{2}}}{\partial t} - \mu_{11} \left(\frac{\partial^{2\nu} u^{n-\frac{1}{2}}}{\partial |x|^{2\nu}} + \frac{\partial^{2\nu} u^{n-\frac{1}{2}}}{\partial |y|^{2\nu}} \right) = f(u^{n-\frac{1}{2}}, v^{n-\frac{1}{2}}) + O(\tau^2), \tag{29}$$

$$\frac{\partial v^{n-\frac{1}{2}}}{\partial t} - \mu_{21} \left(\frac{\partial^{2\eta} v^{n-\frac{1}{2}}}{\partial |x|^{2\eta}} + \frac{\partial^{2\eta} v^{n-\frac{1}{2}}}{\partial |y|^{2\eta}} \right) = g(u^{n-\frac{1}{2}}, v^{n-\frac{1}{2}}) + O(\tau^2). \tag{30}$$

From the above relations, the use of the Crank-Nicolson finite difference idea gives:

$$\frac{u^n - u^{n-1}}{\tau} - \frac{\mu_{11}}{2} \left(\frac{\partial^{2\nu} u^n}{\partial |x|^{2\nu}} + \frac{\partial^{2\nu} u^{n-1}}{\partial |x|^{2\nu}} + \frac{\partial^{2\nu} u^n}{\partial |y|^{2\nu}} + \frac{\partial^{2\nu} u^{n-1}}{\partial |y|^{2\nu}} \right) = f(u^{n-\frac{1}{2}}, v^{n-\frac{1}{2}}) + O(\tau^2), \tag{31}$$

$$\frac{v^n - v^{n-1}}{\tau} - \frac{\mu_{22}}{2} \left(\frac{\partial^{2\eta} v^n}{\partial |x|^{2\eta}} + \frac{\partial^{2\eta} v^{n-1}}{\partial |x|^{2\eta}} + \frac{\partial^{2\eta} v^n}{\partial |y|^{2\eta}} + \frac{\partial^{2\eta} v^{n-1}}{\partial |y|^{2\eta}} \right) = g(u^{n-\frac{1}{2}}, v^{n-\frac{1}{2}}) + O(\tau^2). \tag{32}$$

or

$$u^n - \frac{\tau\mu_{11}}{2} \frac{\partial^{2\nu} u^n}{\partial|x|^{2\nu}} - \frac{\tau\mu_{11}}{2} \frac{\partial^{2\nu} u^n}{\partial|y|^{2\nu}} \tag{33}$$

$$= u^{n-1} + \frac{\tau\mu_{11}}{2} \frac{\partial^{2\nu} u^{n-1}}{\partial|x|^{2\nu}} + \frac{\tau\mu_{11}}{2} \frac{\partial^{2\nu} u^{n-1}}{\partial|y|^{2\nu}} + \tau f(u^{n-\frac{1}{2}}, v^{n-\frac{1}{2}}) + O(\tau^2),$$

$$v^n - \frac{\tau\mu_{22}}{2} \frac{\partial^{2\eta} v^n}{\partial|x|^{2\eta}} - \frac{\tau\mu_{22}}{2} \frac{\partial^{2\eta} v^n}{\partial|y|^{2\eta}} \tag{34}$$

$$= v^{n-1} + \frac{\tau\mu_{22}}{2} \frac{\partial^{2\eta} v^{n-1}}{\partial|x|^{2\eta}} + \frac{\tau\mu_{22}}{2} \frac{\partial^{2\eta} v^{n-1}}{\partial|y|^{2\eta}} + \tau g(u^{n-\frac{1}{2}}, v^{n-\frac{1}{2}}) + O(\tau^2).$$

Omitting the small term $O(\tau^2)$ from the above relation results

$$\tilde{u}^n - \frac{\tau\mu_{11}}{2} \frac{\partial^{2\nu} \tilde{u}^n}{\partial|x|^{2\nu}} - \frac{\tau\mu_{11}}{2} \frac{\partial^{2\nu} \tilde{u}^n}{\partial|y|^{2\nu}} = \tilde{u}^{n-1} + \frac{\tau\mu_{11}}{2} \frac{\partial^{2\nu} \tilde{u}^{n-1}}{\partial|x|^{2\nu}} + \frac{\tau\mu_{11}}{2} \frac{\partial^{2\nu} \tilde{u}^{n-1}}{\partial|y|^{2\nu}} + \tau f(\tilde{u}^{n-\frac{1}{2}}, \tilde{v}^{n-\frac{1}{2}}), \tag{35}$$

$$\tilde{v}^n - \frac{\tau\mu_{22}}{2} \frac{\partial^{2\eta} \tilde{v}^n}{\partial|x|^{2\eta}} - \frac{\tau\mu_{22}}{2} \frac{\partial^{2\eta} \tilde{v}^n}{\partial|y|^{2\eta}} = \tilde{v}^{n-1} + \frac{\tau\mu_{22}}{2} \frac{\partial^{2\eta} \tilde{v}^{n-1}}{\partial|x|^{2\eta}} + \frac{\tau\mu_{22}}{2} \frac{\partial^{2\eta} \tilde{v}^{n-1}}{\partial|y|^{2\eta}} + \tau g(\tilde{u}^{n-\frac{1}{2}}, \tilde{v}^{n-\frac{1}{2}}). \tag{36}$$

According to Eq. (36), we want to find $\tilde{u}^n, \tilde{v}^n \in H_0^\beta(\Omega) \cap C^0(\Omega)$ such that

$$\langle \tilde{u}^n, \zeta_1 \rangle + \frac{\tau\mu_{11}}{2} \mathbb{Q}_1(\tilde{u}^n, \zeta_1) = \langle \tilde{u}^{n-1}, \zeta_1 \rangle - \frac{\tau\mu_{11}}{2} \mathbb{Q}_1(\tilde{u}^{n-1}, \zeta_1) + \tau \langle f(\tilde{u}^{n-\frac{1}{2}}, \tilde{v}^{n-\frac{1}{2}}), \zeta_1 \rangle, \tag{37}$$

$$\langle \tilde{v}^n, \zeta_2 \rangle + \frac{\tau\mu_{22}}{2} \mathbb{Q}_2(\tilde{v}^n, \zeta_2) = \langle \tilde{v}^{n-1}, \zeta_2 \rangle - \frac{\tau\mu_{22}}{2} \mathbb{Q}_2(\tilde{v}^{n-1}, \zeta_2) + \tau \langle g(\tilde{u}^{n-\frac{1}{2}}, \tilde{v}^{n-\frac{1}{2}}), \zeta_2 \rangle, \tag{38}$$

for every $\zeta_1, \zeta_2 \in H_0^\beta(\Omega) \cap C^0(\Omega)$ where $\langle \cdot, \cdot \rangle$ denotes the inner product and

$$\mathbb{Q}_1(\Phi^n, \zeta_1) = \mu_{11} \left[({}^R D_x^\nu \Phi^n, {}^R D_b^\nu \zeta_1) + ({}^R D_b^\nu \Phi^n, {}^R D_x^\nu \zeta_1) \right] \tag{39}$$

$$+ \mu_{11} \left[({}^R D_y^\nu \Phi^n, {}^R D_d^\nu \zeta_1) + ({}^R D_d^\nu \Phi^n, {}^R D_y^\nu \zeta_1) \right],$$

$$\mathbb{Q}_2(\Phi^n, \zeta_2) = \mu_{22} \left[({}^R D_x^\eta \Phi^n, {}^R D_b^\eta \zeta_2) + ({}^R D_b^\eta \Phi^n, {}^R D_x^\eta \zeta_2) \right] \tag{40}$$

$$+ \mu_{22} \left[({}^R D_y^\eta \Phi^n, {}^R D_d^\eta \zeta_2) + ({}^R D_d^\eta \Phi^n, {}^R D_y^\eta \zeta_2) \right].$$

Theorem 3.1. Let $\tilde{u}^n, \tilde{v}^n \in H_0^\beta(\Omega) \cap C^0(\Omega)$. So, Equation (36) is unconditionally stable.

Proof. The roundoff error equation for relation (36) is as follows

$$\langle \Xi_1^n, \zeta_1 \rangle + \frac{\tau\mu_{11}}{2} \mathbb{Q}_1(\Xi_1^n, \zeta_1) = \langle \Xi_1^{n-1}, \zeta_1 \rangle - \frac{\tau\mu_{11}}{2} \mathbb{Q}_1(\Xi_1^{n-1}, \zeta_1) + \tau \langle f(u^n, v^n) - f(\tilde{u}^n, \tilde{v}^n), \zeta_1 \rangle \tag{41}$$

$$\langle \Xi_2^n, \zeta_2 \rangle + \frac{\tau\mu_{22}}{2} \mathbb{Q}_2(\Xi_2^n, \zeta_2) = \langle \Xi_2^{n-1}, \zeta_2 \rangle - \frac{\tau\mu_{22}}{2} \mathbb{Q}_2(\Xi_2^{n-1}, \zeta_2) + \tau \langle g(u^n, v^n) - g(\tilde{u}^n, \tilde{v}^n), \zeta_2 \rangle, \tag{42}$$

where $\Xi_1^n = \tilde{u}^n - \bar{u}^n$ and $\Xi_2^n = \tilde{v}^n - \bar{v}^n$. Also, \bar{u}^n and \bar{v}^n are approximate values of \tilde{u}^n and \tilde{v}^n , respectively. Now, we put $\zeta_1 = \Xi_1^n$ and $\zeta_2 = \Xi_2^n$ in relation (41) that it gives

$$\begin{aligned} \langle \Xi_1^n, \Xi_1^n \rangle &+ \frac{\tau\mu_{11}}{2} Q_1(\Xi_1^n, \Xi_1^n) \\ &= \langle \Xi_1^{n-1}, \zeta_1 \rangle - \frac{\tau\mu_{11}}{2} Q_1(\Xi_1^{n-1}, \Xi_1^n) + \tau \langle f(u^n, v^n) - f(\tilde{u}^n, \tilde{v}^n), \Xi_1^n \rangle, \end{aligned} \quad (43)$$

$$\begin{aligned} \langle \Xi_2^n, \Xi_2^n \rangle &+ \frac{\tau\mu_{22}}{2} Q_2(\Xi_2^n, \Xi_2^n) \\ &= \langle \Xi_2^{n-1}, \Xi_2^n \rangle - \frac{\tau\mu_{22}}{2} Q_2(\Xi_2^{n-1}, \Xi_2^n) + \tau \langle g(u^n, v^n) - g(\tilde{u}^n, \tilde{v}^n), \Xi_2^n \rangle, \end{aligned} \quad (44)$$

From Theorem 1 of Ref. [52] we obtain

$$Q_1(\Xi_1^n, \Xi_1^n) \geq \mu_{11} \|\Xi_1^n\|_{H^\beta(\Omega)}^2, \quad (45)$$

$$Q_2(\Xi_2^n, \Xi_2^n) \geq \mu_{22} \|\Xi_2^n\|_{H^\beta(\Omega)}^2. \quad (46)$$

Here, for the nonlinear relation, we can get

$$\langle f(u^n, v^n) - f(\tilde{u}^n, \tilde{v}^n), \Xi_1^n \rangle \leq \langle L \|u^n - \tilde{u}^n\| + L \|v^n - \tilde{v}^n\|, \Xi_1^n \rangle \leq \langle L_1 \|\Xi_1^n\| + L_1 \|\Xi_2^n\|, \Xi_1^n \rangle, \quad (47)$$

$$\langle g(u^n, v^n) - g(\tilde{u}^n, \tilde{v}^n), \Xi_2^n \rangle \leq \langle L \|u^n - \tilde{u}^n\| + L \|v^n - \tilde{v}^n\|, \Xi_2^n \rangle \leq \langle L_2 \|\Xi_1^n\| + L_2 \|\Xi_2^n\|, \Xi_2^n \rangle. \quad (48)$$

Now, from Equations (43) and (44) we can write

$$\begin{aligned} \|\Xi_1^n\|_{L^2(\Omega)}^2 &+ \frac{C\tau\mu_{11}}{2} \|\Xi_1^n\|_{H^\nu(\Omega)}^2 \leq \|\Xi_1^{n-1}\|_{L^2(\Omega)} \|\Xi_1^n\|_{L^2(\Omega)} + C \frac{\tau\mu_{11}}{2} \|\Xi_1^{n-1}\|_{H^\nu(\Omega)} \|\Xi_1^n\|_{H^\nu(\Omega)} \\ &+ \tau L_1 \left(\|\Xi_1^n\|_{H^\nu(\Omega)} + \|\Xi_2^n\|_{H^\nu(\Omega)} \right) \|\Xi_1^n\|_{H^\nu(\Omega)}, \end{aligned} \quad (49)$$

$$\begin{aligned} \|\Xi_2^n\|_{L^2(\Omega)}^2 &+ \frac{\tau\mu_{22}}{2} \|\Xi_2^n\|_{H^\nu(\Omega)}^2 \leq \|\Xi_2^{n-1}\|_{L^2(\Omega)} \|\Xi_2^n\|_{L^2(\Omega)} + \frac{C\tau\mu_{22}}{2} \|\Xi_2^{n-1}\|_{H^\nu(\Omega)} \|\Xi_2^n\|_{H^\nu(\Omega)} \\ &+ \tau L_2 \left(\|\Xi_1^n\|_{H^\nu(\Omega)} + \|\Xi_2^n\|_{H^\nu(\Omega)} \right) \|\Xi_2^n\|_{H^\nu(\Omega)}. \end{aligned} \quad (50)$$

According to the previous relation, the following relations can be obtained

$$\begin{aligned} \|\Xi_1^n\|_{L^2(\Omega)}^2 &+ \frac{C\tau\mu_{11}}{2} \|\Xi_1^n\|_{H^\nu(\Omega)}^2 \leq \frac{1}{2} \|\Xi_1^{n-1}\|_{L^2(\Omega)}^2 + \frac{1}{2} \|\Xi_1^n\|_{L^2(\Omega)}^2 + C \frac{\tau\mu_{11}}{4} \|\Xi_1^{n-1}\|_{H^\nu(\Omega)}^2 \\ &+ C \frac{\tau\mu_{11}}{4} \|\Xi_1^n\|_{H^\nu(\Omega)}^2 + \tau L_1 \left(\|\Xi_1^n\|_{L^2(\Omega)} + \|\Xi_2^n\|_{L^2(\Omega)} \right) \|\Xi_1^n\|_{L^2(\Omega)}, \end{aligned} \quad (51)$$

$$\begin{aligned} \|\Xi_2^n\|_{L^2(\Omega)}^2 &+ \frac{C\tau\mu_{22}}{2} \|\Xi_2^n\|_{H^\nu(\Omega)}^2 \leq \frac{1}{2} \|\Xi_2^{n-1}\|_{L^2(\Omega)}^2 + \frac{1}{2} \|\Xi_2^n\|_{L^2(\Omega)}^2 + C \frac{\tau\mu_{22}}{4} \|\Xi_2^{n-1}\|_{H^\nu(\Omega)}^2 \\ &+ C \frac{\tau\mu_{22}}{4} \|\Xi_2^n\|_{H^\nu(\Omega)}^2 + \tau L_2 \left(\|\Xi_1^n\|_{L^2(\Omega)} + \|\Xi_2^n\|_{L^2(\Omega)} \right) \|\Xi_2^n\|_{L^2(\Omega)}. \end{aligned} \quad (52)$$

The simplified form of Equations (51) and (52) are

$$\begin{aligned} \frac{1}{2} \|\Xi_1^n\|_{L^2(\Omega)}^2 + \frac{C\tau\mu_{11}}{4} \|\Xi_1^n\|_{H^\nu(\Omega)}^2 &\leq \frac{1}{2} \|\Xi_1^{n-1}\|_{L^2(\Omega)}^2 + C\frac{\tau\mu_{11}}{4} \|\Xi_1^{n-1}\|_{H^\nu(\Omega)}^2 \\ &+ \tau L_1 \|\Xi_1^n\|_{L^2(\Omega)}^2 + \frac{\tau L_1}{2} \|\Xi_2^n\|_{L^2(\Omega)}^2 + \frac{\tau L_1}{2} \|\Xi_1^n\|_{L^2(\Omega)}^2, \\ \frac{1}{2} \|\Xi_2^n\|_{L^2(\Omega)}^2 + \frac{C\tau\mu_{22}}{4} \|\Xi_2^n\|_{H^\eta(\Omega)}^2 &\leq \frac{1}{2} \|\Xi_2^{n-1}\|_{L^2(\Omega)}^2 + C\frac{\tau\mu_{22}}{4} \|\Xi_2^{n-1}\|_{H^\eta(\Omega)}^2 \\ &+ \frac{\tau L_1}{2} \|\Xi_1^n\|_{L^2(\Omega)}^2 + \frac{\tau L_1}{2} \|\Xi_2^n\|_{L^2(\Omega)}^2 + \tau L_2 \|\Xi_2^n\|_{L^2(\Omega)}^2. \end{aligned}$$

Changing index n to j and summing the above relation for $j = 0$ to n , give

$$\begin{aligned} \|\Xi_1^n\|_{L^2(\Omega)}^2 + \frac{C\tau\mu_{11}}{2} \|\Xi_1^n\|_{H^\nu(\Omega)}^2 &\leq \|\Xi_1^0\|_{L^2(\Omega)}^2 + \frac{C\tau\mu_{11}}{2} \|\Xi_1^0\|_{H^\nu(\Omega)}^2 \\ &+ 3\tau L_1 \sum_{j=0}^n \|\Xi_1^j\|_{L^2(\Omega)}^2 + \tau L_1 \sum_{j=0}^n \|\Xi_2^j\|_{L^2(\Omega)}^2, \end{aligned} \quad (53)$$

$$\begin{aligned} \|\Xi_2^n\|_{L^2(\Omega)}^2 + \frac{C\tau\mu_{22}}{2} \|\Xi_2^n\|_{H^\eta(\Omega)}^2 &\leq \|\Xi_2^0\|_{L^2(\Omega)}^2 + \frac{C\tau\mu_{22}}{2} \|\Xi_2^0\|_{H^\eta(\Omega)}^2 \\ &+ 3\tau L_2 \sum_{j=0}^n \|\Xi_2^j\|_{L^2(\Omega)}^2 + \tau L_2 \sum_{j=0}^n \|\Xi_1^j\|_{L^2(\Omega)}^2. \end{aligned} \quad (54)$$

Summing Equations (53) with (54), results

$$\begin{aligned} \|\Xi_1^n\|_{L^2(\Omega)}^2 + \|\Xi_2^n\|_{L^2(\Omega)}^2 &\leq \left(\frac{1+3\tau L}{1-3\tau L} \right) \left[\|\Xi_1^0\|_{L^2(\Omega)}^2 + \|\Xi_2^0\|_{L^2(\Omega)}^2 \right] \\ &+ \left(\frac{1+3\tau L}{1-3\tau L} \right) \left[\sum_{j=1}^n \|\Xi_1^j\|_{L^2(\Omega)}^2 + \sum_{j=1}^n \|\Xi_2^j\|_{L^2(\Omega)}^2 \right] \\ &\leq \left(\frac{1+3\tau L}{1-3\tau L} \right) \left[\|\Xi_1^0\|_{L^2(\Omega)}^2 + \|\Xi_2^0\|_{L^2(\Omega)}^2 \right] \exp \left(n \left(\frac{1+3\tau L}{1-3\tau L} \right) \right) \\ &\leq \left(\frac{1+3\tau L}{1-3\tau L} \right) \left[\|\Xi_1^0\|_{L^2(\Omega)}^2 + \|\Xi_2^0\|_{L^2(\Omega)}^2 \right] \exp \left(\left(\frac{1+3\tau L}{1-3\tau L} \right)^n \right). \end{aligned} \quad (55)$$

If $n \rightarrow \infty$ then

$$\begin{aligned} \|\Xi_1^n\|_{L^2(\Omega)}^2 + \|\Xi_2^n\|_{L^2(\Omega)}^2 &\leq \left(\frac{1+3\tau L}{1-3\tau L} \right) \left[\|\Xi_1^0\|_{L^2(\Omega)}^2 + \|\Xi_2^0\|_{L^2(\Omega)}^2 \right] \exp(\exp(9T\mathcal{L})) \\ &\leq C(\mathcal{L}, T) \left[\|\Xi_1^0\|_{L^2(\Omega)}^2 + \|\Xi_2^0\|_{L^2(\Omega)}^2 \right], \end{aligned} \quad (56)$$

thus

$$\|\Xi_1^n\|_{L^2(\Omega)}^2 + \|\Xi_2^n\|_{L^2(\Omega)}^2 \leq C(\mathcal{L}, T) \left[\|\Xi_1^0\|_{L^2(\Omega)}^2 + \|\Xi_2^0\|_{L^2(\Omega)}^2 \right]. \quad (57)$$

■

Theorem 3.2. Let $u^n, v^n, \tilde{u}^n, \tilde{v}^n \in H_0^\beta(\Omega) \cap C^0(\Omega)$ be solutions of the exact and approximate formulation. So, the time-discrete scheme is convergent and also

$$\|u^n - \tilde{u}^n\|_{H^\beta(\Omega)} \leq C(L, T)\tau^2, \quad \|v^n - \tilde{v}^n\|_{H^\beta(\Omega)} \leq C(L, T)\tau^2.$$

Proof. The proof is similar to the proof of [Theorem 3.1](#). ■

Consider the following approximate solutions

$$\tilde{u}_N^n(x, y) = \sum_{k=0}^N \sum_{m=0}^N u_{k,m}^n \mathcal{J}_k^{-\varpi_1, -\varpi_2}(x) \mathcal{J}_m^{-\varpi_1, -\varpi_2}(y), \quad (58)$$

$$\tilde{v}_N^n(x, y) = \sum_{k=0}^N \sum_{m=0}^N v_{k,m}^n \mathcal{J}_k^{-\varpi_1, -\varpi_2}(x) \mathcal{J}_m^{-\varpi_1, -\varpi_2}(y). \quad (59)$$

Substituting relations (58) and (59) in Equations (35) and (36), give

$$\begin{aligned} \tilde{u}_N^n - \frac{\tau\mu_{11}}{2} \frac{\partial^{2\nu} \tilde{u}_N^n}{\partial|x|^{2\nu}} - \frac{\tau\mu_{11}}{2} \frac{\partial^{2\nu} \tilde{u}_N^n}{\partial|y|^{2\nu}} &= \tilde{u}_N^{n-1} + \frac{\tau\mu_{11}}{2} \frac{\partial^{2\nu} \tilde{u}_N^{n-1}}{\partial|x|^{2\nu}} \\ &+ \frac{\tau\mu_{11}}{2} \frac{\partial^{2\nu} \tilde{u}_N^{n-1}}{\partial|y|^{2\nu}} + \tau f(\tilde{u}_N^{n-\frac{1}{2}}, \tilde{v}_N^{n-\frac{1}{2}}), \end{aligned} \quad (60)$$

$$\begin{aligned} \tilde{v}_N^n - \frac{\tau\mu_{22}}{2} \frac{\partial^{2\eta} \tilde{v}_N^n}{\partial|x|^{2\eta}} - \frac{\tau\mu_{22}}{2} \frac{\partial^{2\eta} \tilde{v}_N^n}{\partial|y|^{2\eta}} &= \tilde{v}_N^{n-1} + \frac{\tau\mu_{22}}{2} \frac{\partial^{2\eta} \tilde{v}_N^{n-1}}{\partial|x|^{2\eta}} \\ &+ \frac{\tau\mu_{22}}{2} \frac{\partial^{2\eta} \tilde{v}_N^{n-1}}{\partial|y|^{2\eta}} + \tau g(\tilde{u}_N^{n-\frac{1}{2}}, \tilde{v}_N^{n-\frac{1}{2}}). \end{aligned} \quad (61)$$

or

$$\begin{aligned} &\sum_{k=0}^N \sum_{m=0}^N u_{k,m}^n \mathcal{J}_k^{-\varpi_1, -\varpi_2}(x) \mathcal{J}_m^{-\varpi_1, -\varpi_2}(y) \\ &- \frac{\tau\mu_{11}}{2} \sum_{k=0}^N \sum_{m=0}^N u_{k,m}^n \frac{\partial^{2\nu}}{\partial|x|^{2\nu}} \mathcal{J}_k^{-\varpi_1, -\varpi_2}(x) \mathcal{J}_m^{-\varpi_1, -\varpi_2}(y) \\ &- \frac{\tau\mu_{11}}{2} \sum_{k=0}^N \sum_{m=0}^N u_{k,m}^n \frac{\partial^{2\nu}}{\partial|y|^{2\nu}} \mathcal{J}_k^{-\varpi_1, -\varpi_2}(x) \mathcal{J}_m^{-\varpi_1, -\varpi_2}(y) \\ &= \sum_{k=0}^N \sum_{m=0}^N u_{k,m}^{n-1} \mathcal{J}_k^{-\varpi_1, -\varpi_2}(x) \mathcal{J}_m^{-\varpi_1, -\varpi_2}(y) \\ &+ \frac{\tau\mu_{11}}{2} \sum_{k=0}^N \sum_{m=0}^N u_{k,m}^{n-1} \frac{\partial^{2\nu}}{\partial|x|^{2\nu}} \mathcal{J}_k^{-\varpi_1, -\varpi_2}(x) \mathcal{J}_m^{-\varpi_1, -\varpi_2}(y) \\ &+ \frac{\tau\mu_{11}}{2} \sum_{k=0}^N \sum_{m=0}^N u_{k,m}^{n-1} \frac{\partial^{2\nu}}{\partial|y|^{2\nu}} \mathcal{J}_k^{-\varpi_1, -\varpi_2}(x) \mathcal{J}_m^{-\varpi_1, -\varpi_2}(y) \\ &+ \tau f\left(\sum_{k=0}^N \sum_{m=0}^N u_{k,m}^{n-\frac{1}{2}} \mathcal{J}_k^{-\varpi_1, -\varpi_2}(x) \mathcal{J}_m^{-\varpi_1, -\varpi_2}(y), \sum_{k=0}^N \sum_{m=0}^N v_{k,m}^{n-\frac{1}{2}} \mathcal{J}_k^{-\varpi_1, -\varpi_2}(x) \mathcal{J}_m^{-\varpi_1, -\varpi_2}(y)\right), \end{aligned} \quad (62)$$

and

$$\begin{aligned}
 & \sum_{k=0}^N \sum_{m=0}^N v_{k,m}^n \mathcal{J}_k^{-\varpi_1, -\varpi_2}(x) \mathcal{J}_m^{-\varpi_1, -\varpi_2}(y) - \frac{\tau \mu_{11}}{2} \sum_{k=0}^N \sum_{m=0}^N v_{k,m}^n \frac{\partial^{2\nu}}{\partial |x|^{2\nu}} \mathcal{J}_k^{-\varpi_1, -\varpi_2}(x) \mathcal{J}_m^{-\varpi_1, -\varpi_2}(y) \\
 & - \frac{\tau \mu_{11}}{2} \sum_{k=0}^N \sum_{m=0}^N v_{k,m}^n \frac{\partial^{2\nu}}{\partial |y|^{2\nu}} \mathcal{J}_k^{-\varpi_1, -\varpi_2}(x) \mathcal{J}_m^{-\varpi_1, -\varpi_2}(y) = \sum_{k=0}^N \sum_{m=0}^N v_{k,m}^{n-1} \mathcal{J}_k^{-\varpi_1, -\varpi_2}(x) \mathcal{J}_m^{-\varpi_1, -\varpi_2}(y) \\
 & + \frac{\tau \mu_{11}}{2} \sum_{k=0}^N \sum_{m=0}^N v_{k,m}^{n-1} \frac{\partial^{2\nu}}{\partial |x|^{2\nu}} \mathcal{J}_k^{-\varpi_1, -\varpi_2}(x) \mathcal{J}_m^{-\varpi_1, -\varpi_2}(y) \\
 & + \frac{\tau \mu_{11}}{2} \sum_{k=0}^N \sum_{m=0}^N v_{k,m}^{n-1} \frac{\partial^{2\nu}}{\partial |y|^{2\nu}} \mathcal{J}_k^{-\varpi_1, -\varpi_2}(x) \mathcal{J}_m^{-\varpi_1, -\varpi_2}(y) \\
 & + \tau f \left(\sum_{k=0}^N \sum_{m=0}^N u_{k,m}^{n-\frac{1}{2}} \mathcal{J}_k^{-\varpi_1, -\varpi_2}(x) \mathcal{J}_m^{-\varpi_1, -\varpi_2}(y), \sum_{k=0}^N \sum_{m=0}^N v_{k,m}^{n-\frac{1}{2}} \mathcal{J}_k^{-\varpi_1, -\varpi_2}(x) \mathcal{J}_m^{-\varpi_1, -\varpi_2}(y) \right). \tag{63}
 \end{aligned}$$

Equations (62) and (63) produce a nonlinear algebraic system of equations which will be solved by the fixed point method.

4 Numerical results

The simulations are performed using MATLAB 2020b software on an Intel(R) Core(TM) i7-4790 CPU @ 3.60GHz, 3.60 GHz with 32 GB of memory.

Consider the mixed patterns on a square

$$\begin{aligned}
 \frac{\partial u}{\partial t} & - \mu_{11} \left(\frac{\partial^{2\nu} u(x, y, t)}{\partial |x|^{2\nu}} + \frac{\partial^{2\nu} u(x, y, t)}{\partial |y|^{2\nu}} \right) = \gamma_1 (\gamma_2 - u + u^2 v), \quad (x, y, t) \in \Omega \times [0, T], \\
 \frac{\partial v}{\partial t} & - \mu_{22} \left(\frac{\partial^{2\eta} u(x, y, t)}{\partial |x|^{2\eta}} + \frac{\partial^{2\eta} u(x, y, t)}{\partial |y|^{2\eta}} \right) = \gamma_1 (\gamma_3 - u^2 v), \quad (x, y, t) \in \Omega \times [0, T], \tag{64}
 \end{aligned}$$

with initial conditions

$$u(x, y, 0) = \text{rand}(0, 1), \quad v(x, y, 0) = \text{rand}(0, 1). \tag{65}$$

Here $\Omega = [0, 20] \times [0, 20]$, 1280 collocation distributed points in the physical domain and $\tau = 10^{-5}$. Here, we consider two different cases:

Case 1:

γ_1	γ_2	γ_3	μ_{11}	μ_{22}
230.82	0.1	0.9	1	8.6676

Figure 2 illustrates L_2 -norm obtained with $\gamma_1 = 230.82, \gamma_2 = 0.1, \gamma_3 = 0.9, \mu_{11} = 0.05, \mu_{22} = 1$ and $2\nu = 2\eta = 1.1$. Furthermore, Figure 3 presents L_2 -norm obtained with $\gamma_1 = 230.82, \gamma_2 = 0.1, \gamma_3 = 0.9, \mu_{11} = 0.05, \mu_{22} = 1$ and $2\nu = 2\eta = 1.5$. Figures 4 to 7, demonstrate the pattern formation with $2\nu = 2\eta = 1.1, 2\nu = 2\eta = 1.5, 2\nu = 2\eta = 1.8$ and $2\nu = 2\eta = 1.9$ respectively. We fixed the constant parameters in the main model and changed the fractional order. The effect of fractional-order can be observed in Figures 4 to 7.

The depicted patterns in Figures 4 to 7 are very different together and each pattern formation can be seen in various phenomena. Figure 4 shows the pattern formation with $2\nu = 2\eta = 1.1$ which the shape of patterns are finger-picking patterns. Figure 5 is obtained with $2\nu = 2\eta = 1.5$ that its shape is parallel uniform lines. The pattern shapes of Figures 6 and 7 with $2\nu = 2\eta = 1.8$ and $2\nu = 2\eta = 1.9$ are elliptical.

Case 2:

γ_1	γ_2	γ_3	μ_{11}	μ_{22}
230.82	0.1	0.9	0.05	1

Figures 8 to 11 illustrate the pattern formation with $2\nu = 2\eta = 1.1$, $2\nu = 2\eta = 1.5$ and $2\nu = 2\eta = 1.8$, respectively. The effect of fractional-order can be observed in Figures 8 to 11. The pattern formations in Figures 8 to 11 have circular shapes whereas the radius of each circular shape is growing by increasing the fractional order.

The numerical results of the proposed method have been compared with the finite difference and finite element methods. The current example does not have any exact solution. Thus, we pursue the following strategy. The obtained solutions with $\tau = 10^{-4}$ and $N = 6000$ collocation points using the present methods are named u^r and v^r as the reference solutions (as an exact solution). Consequently, we use the numerical procedure with $\tau = 10^{-4}$ and different values of N_i to obtain u^{N_i} and v^{N_i} (numerical solutions applying the method presented in the current paper). Now, by interpolating the reference solution at N_i points, we obtain the numerical solutions u^I and v^I (numerical solutions using interpolating). Finally, we define the following error relations

$$\begin{aligned}\mathcal{E}_{u,\infty}^N &= \|u^I - u^{N_i}\|_{\infty}, \\ \mathcal{E}_{v,\infty}^N &= \|v^I - v^{N_i}\|_{\infty}.\end{aligned}$$

For further explanation, follow the below commands

- Compute u^e with $N = 6000$ and $\tau = 10^{-4}$,
- Compute u^{N_i} with $N_i = 200$ and $\tau = 10^{-4}$,
- x -coordinate and y -coordinate denote $N = 6000$ distributed nodes,
- x_{200} -coordinate and y_{200} -coordinate denote $N = 200$ distributed nodes,
- $u^I =$ Interpolate u^e on nodes x_{200} and y_{200} ,
- $\mathcal{E}_{\Pi,\infty}^N = \|u^I - u^{N_i}\|_{\infty}$.

In the finite difference scheme, the reference solution is constructed based on 6000 equally spaced points. Also, the reference solution of the finite element method is obtained with 438 triangle elements. Tables 1 and 2 present the error obtained based on the reference solution for cases 1 and 2, respectively.

5 Conclusion and future works

Here, the effect of fractional order derivative is studied via the Jacobi fractional collocation method. The proposed numerical solution is based on combining the finite difference method and fractional collocation technique. In the first step, the time derivative is discretized by

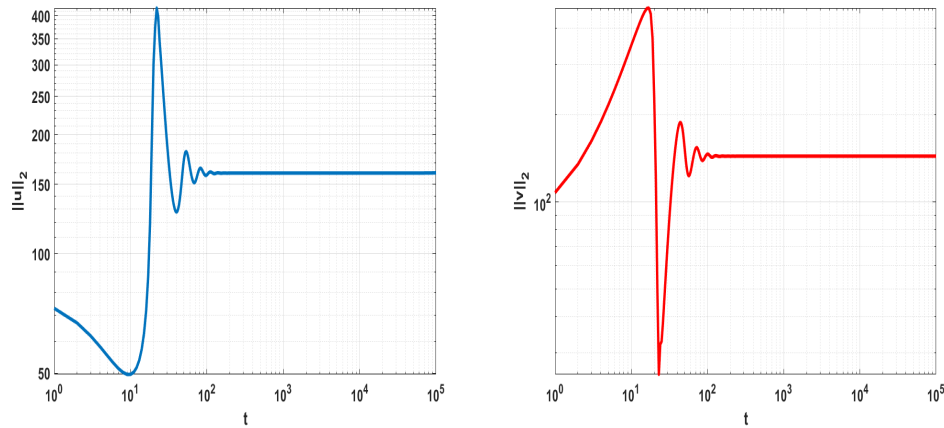


Figure 2: L_2 -norm obtained with $\gamma_1 = 230.82$, $\gamma_2 = 0.1$, $\gamma_3 = 0.9$, $\mu_{11} = 0.05$, $\mu_{22} = 1$ and $2\nu = 2\eta = 1.1$

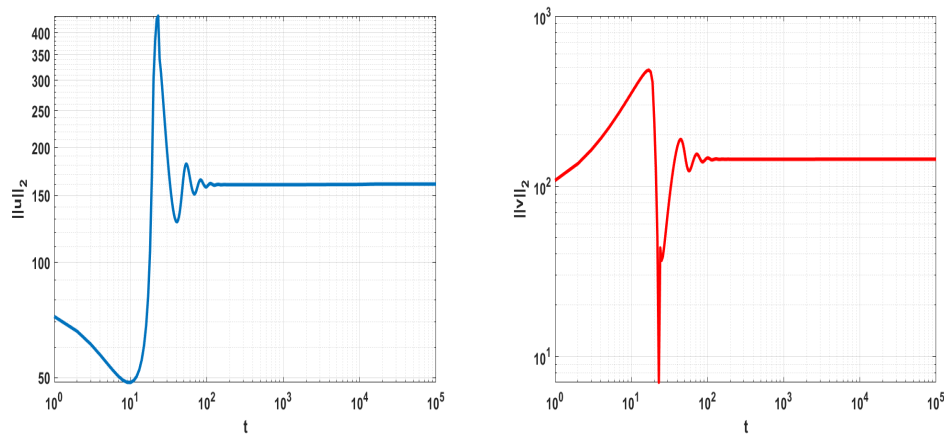


Figure 3: L_2 -norm obtained with $\gamma_1 = 230.82$, $\gamma_2 = 0.1$, $\gamma_3 = 0.9$, $\mu_{11} = 0.05$, $\mu_{22} = 1$ and $2\nu = 2\eta = 1.5$.

a second-order difference scheme. The stability analysis and convergence rate of the time-discrete method are analytically investigated. In the second attempt, the full-discrete plan is constructed. In the numerical experiments, we fixed all constant parameters and displayed pattern formations based on the various fractional orders. It must be noted that the spectral method has high accuracy but it can be applied to the rectangular physical domain, easily. Furthermore, in the future, we want to consider the time- and space-fractional Brusselator model and study the effect of fractional orders of time and space derivatives.

Conflicts of Interest. The authors declare that they have no conflicts of interest regarding the publication of this article.

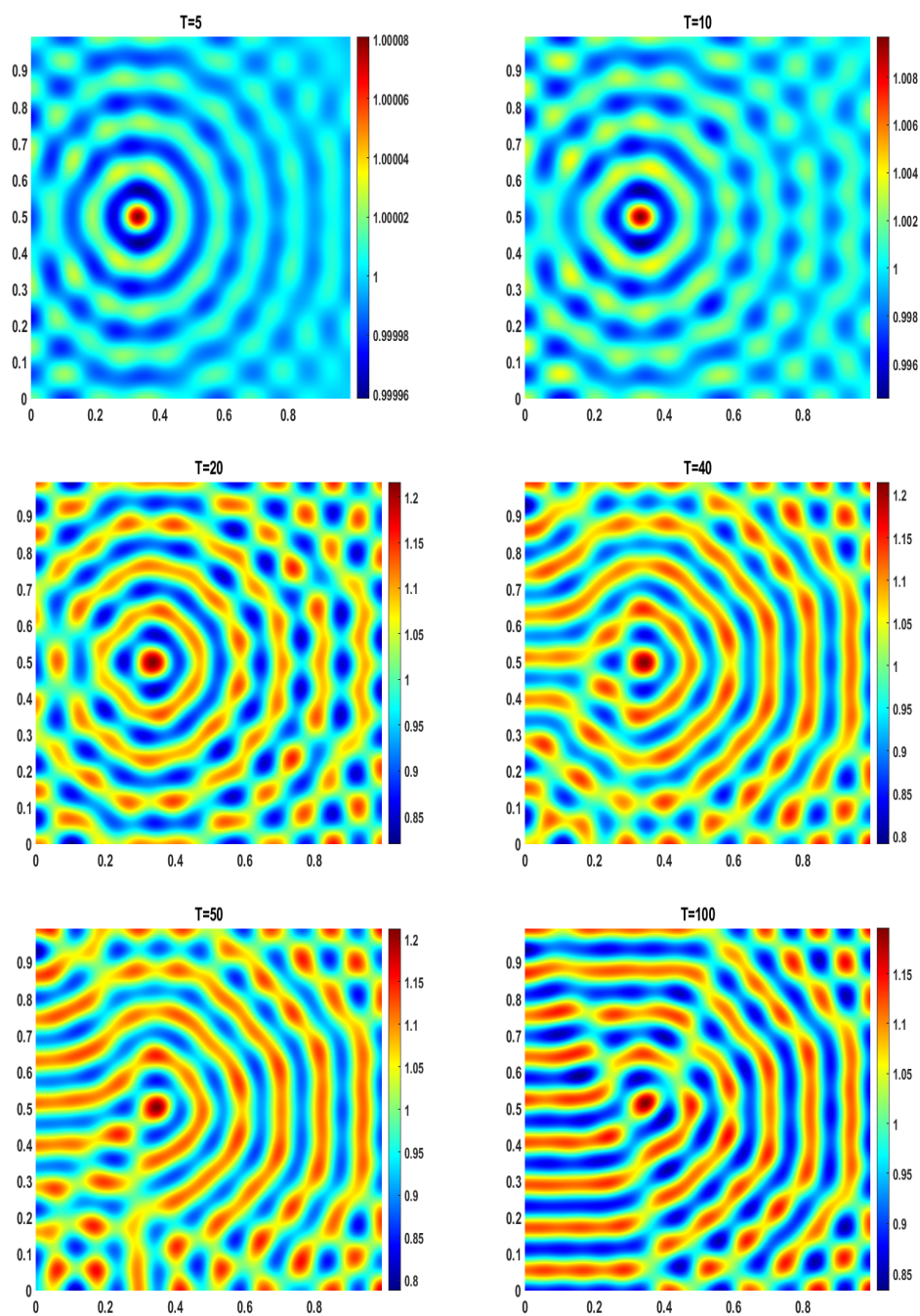


Figure 4: Pattern formation with $\gamma_1=230.82$, $\gamma_2=0.1$, $\gamma_3=0.9$, $\mu_{11}=1$, $\mu_{22}=8.6676$ and $2\nu=2\eta=1.1$.

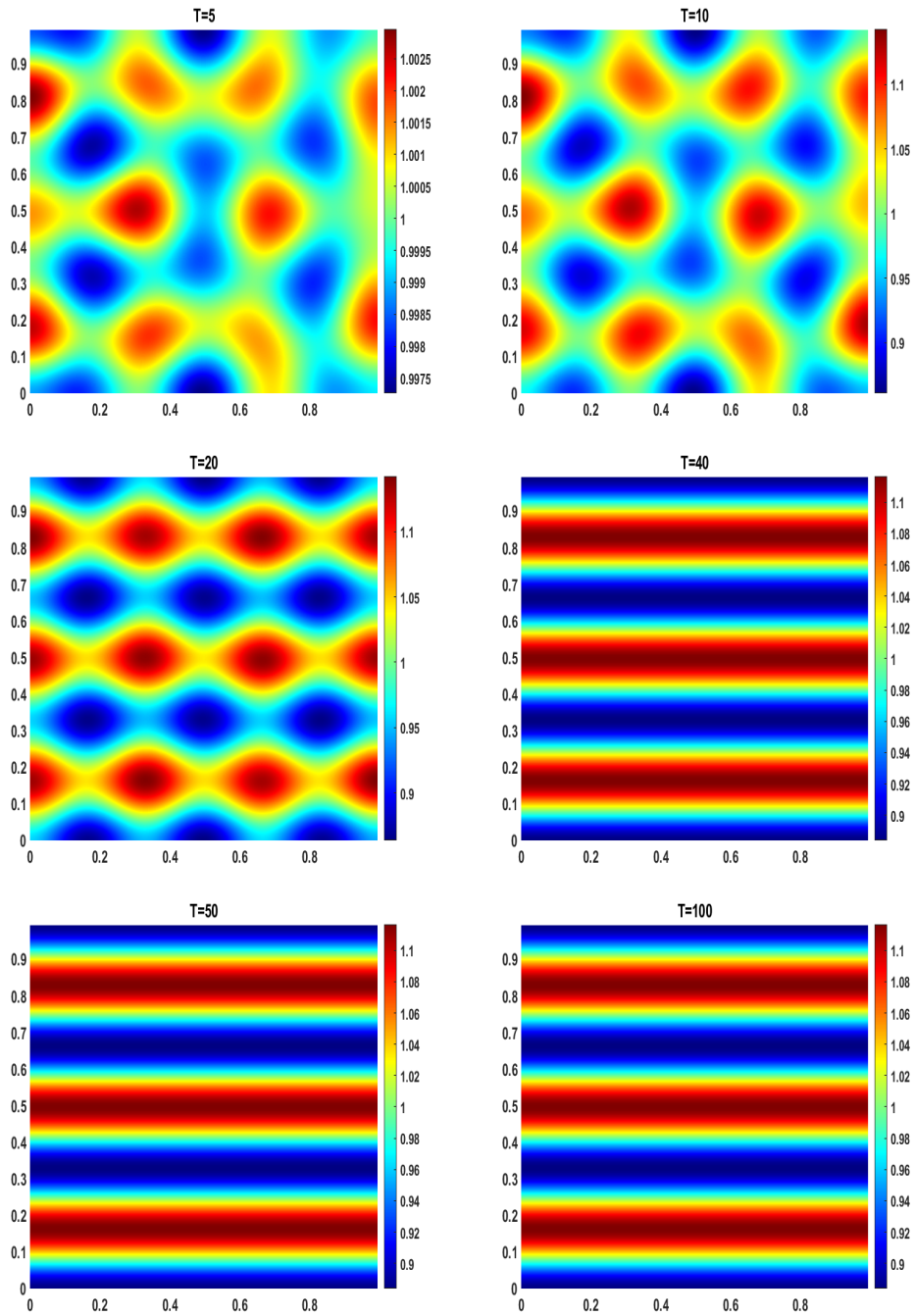


Figure 5: Pattern formation with $\gamma_1=230.82$, $\gamma_2=0.1$, $\gamma_3=0.9$, $\mu_{11}=1$, $\mu_{22}=8.6676$ and $2\nu=2\eta=1.5$.

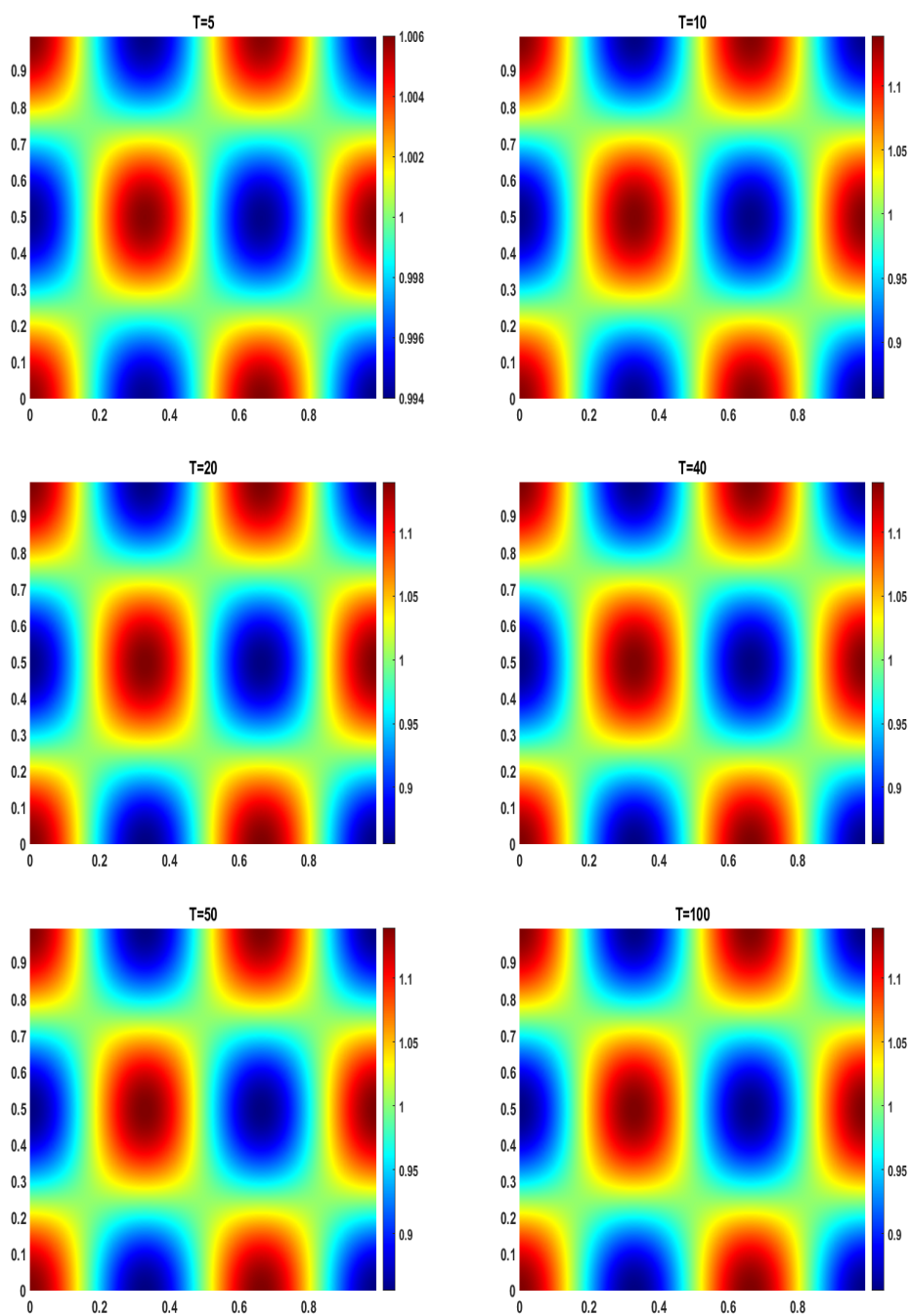


Figure 6: Pattern formation with $\gamma_1=230.82$, $\gamma_2=0.1$, $\gamma_3=0.9$, $\mu_{11}=1$, $\mu_{22}=8.6676$ and $2\nu=2\eta=1.8$.

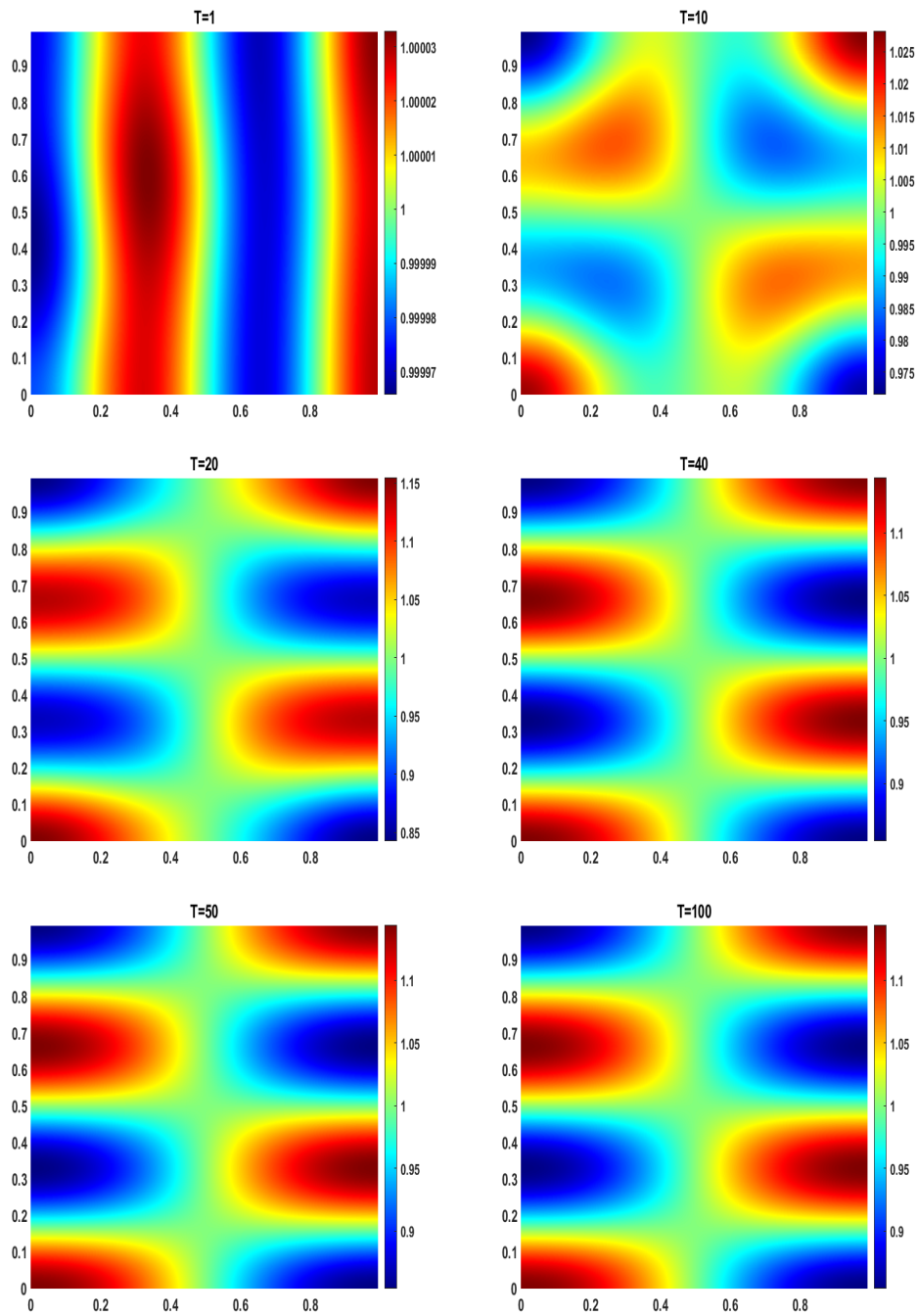


Figure 7: Pattern formation with $\gamma_1=230.82$, $\gamma_2=0.1$, $\gamma_3=0.9$, $\mu_{11}=1$, $\mu_{22}=8.6676$ and $2\nu=2\eta=1.9$.

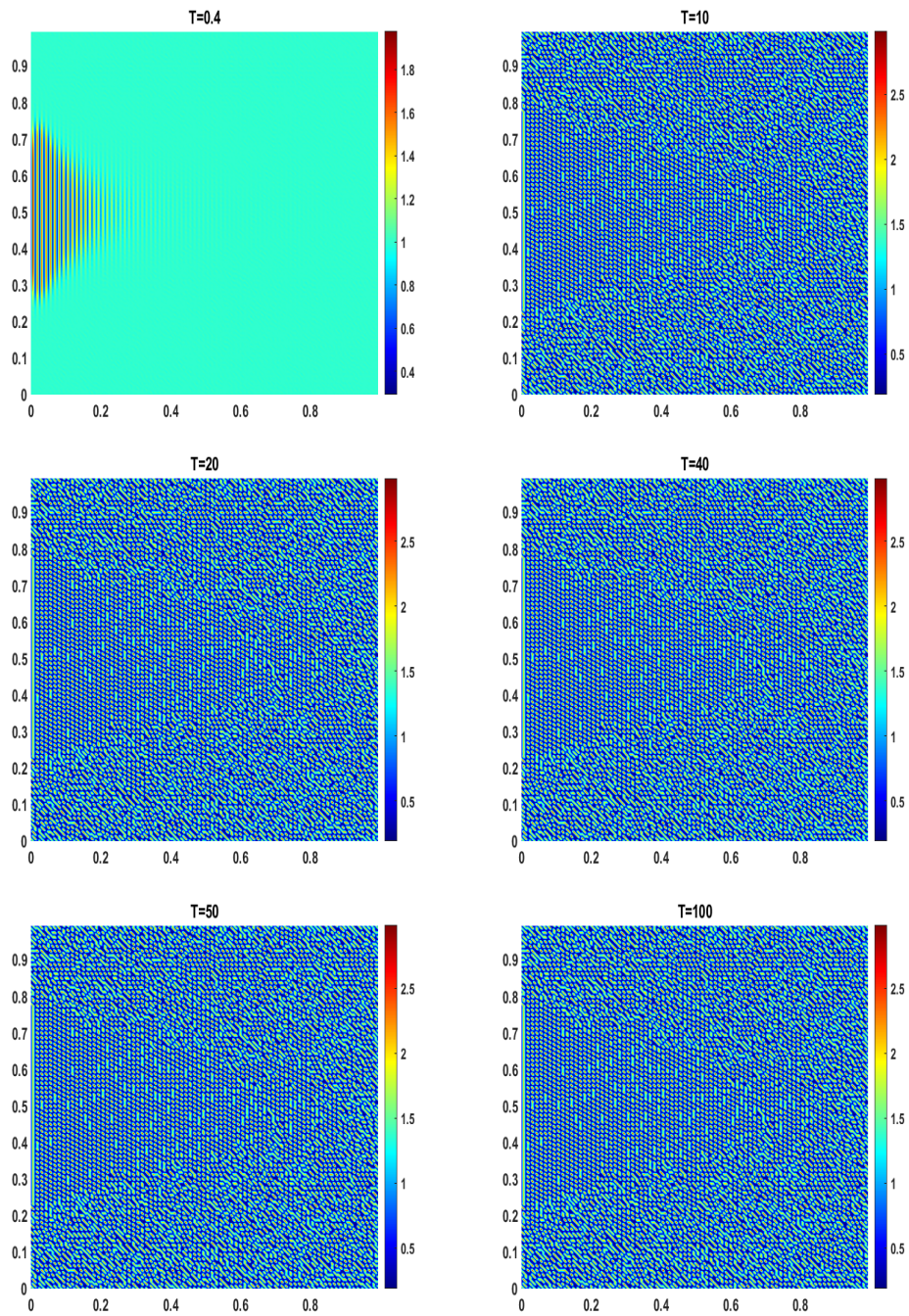


Figure 8: Pattern formation with $\gamma_1 = 230.82$, $\gamma_2 = 0.1$, $\gamma_3 = 0.9$, $\mu_{11} = 0.05$, $\mu_{22} = 1$ and $2\nu = 2\eta = 1.1$.

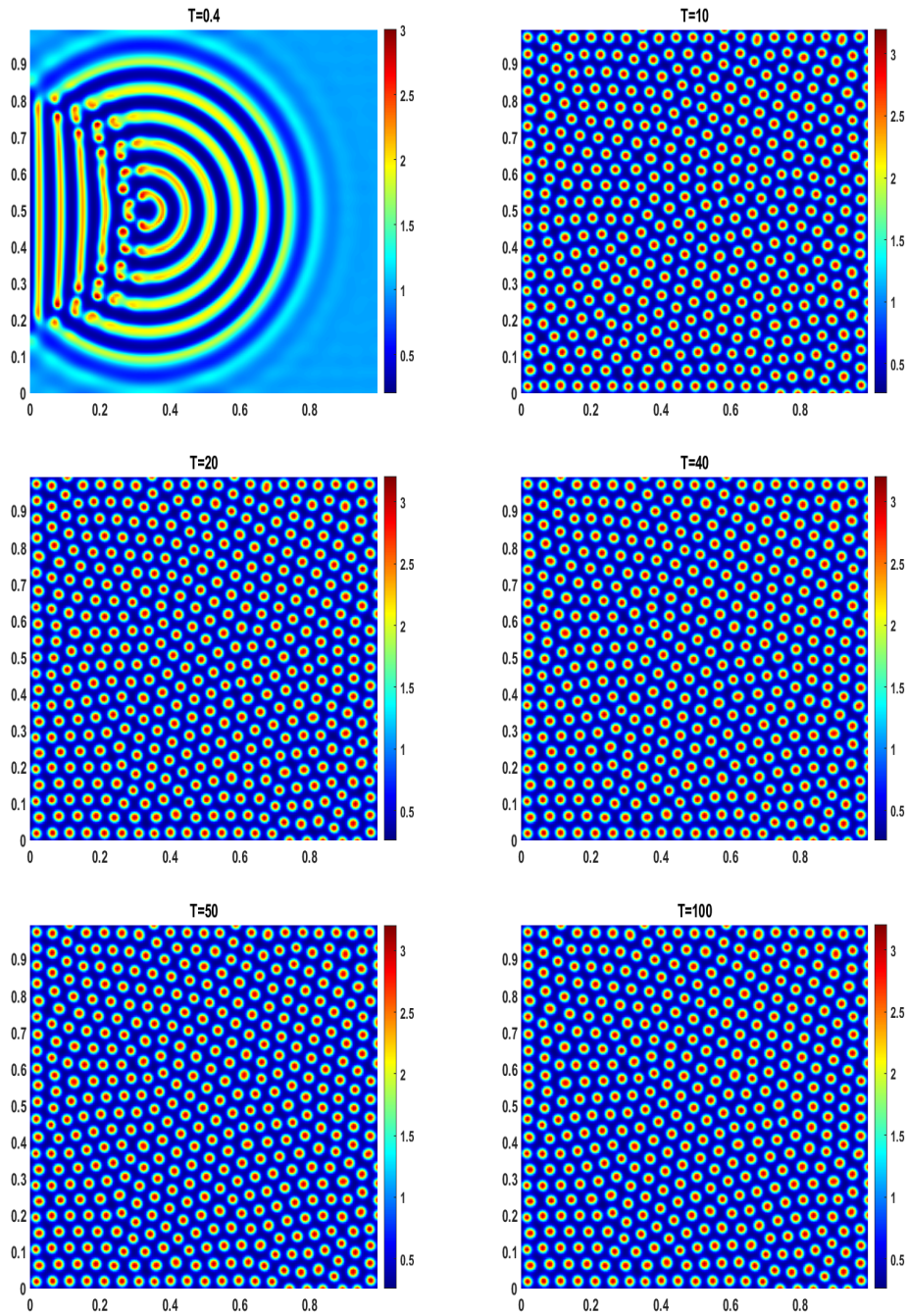


Figure 9: Pattern formation with $\gamma_1 = 230.82$, $\gamma_2 = 0.1$, $\gamma_3 = 0.9$, $\mu_{11} = 0.05$, $\mu_{22} = 1$ and $2\nu = 2\eta = 1.5$.

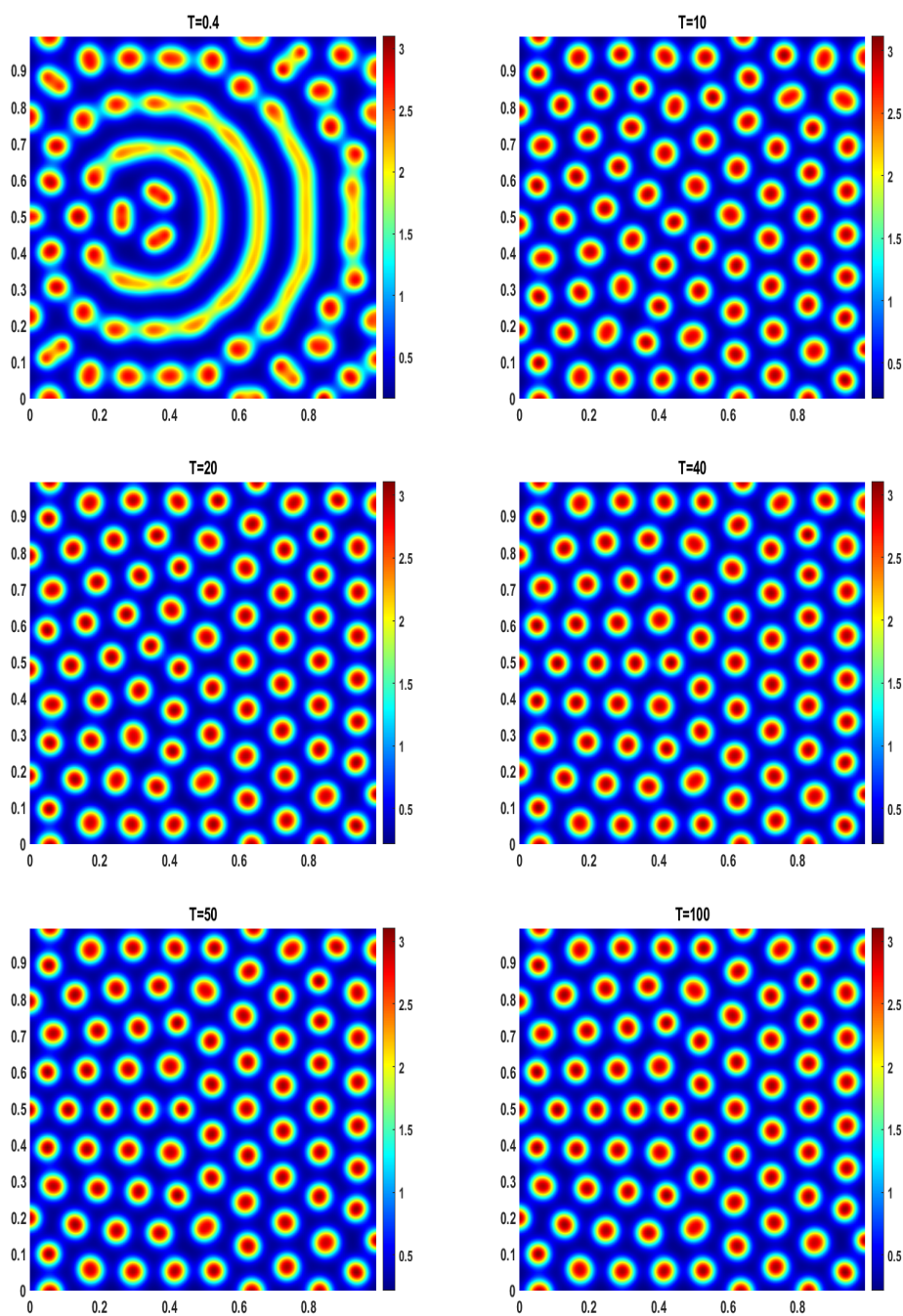


Figure 10: Pattern formation with $\gamma_1 = 230.82$, $\gamma_2 = 0.1$, $\gamma_3 = 0.9$, $\mu_{11} = 0.05$, $\mu_{22} = 1$ and $2\nu = 2\eta = 1.8$.

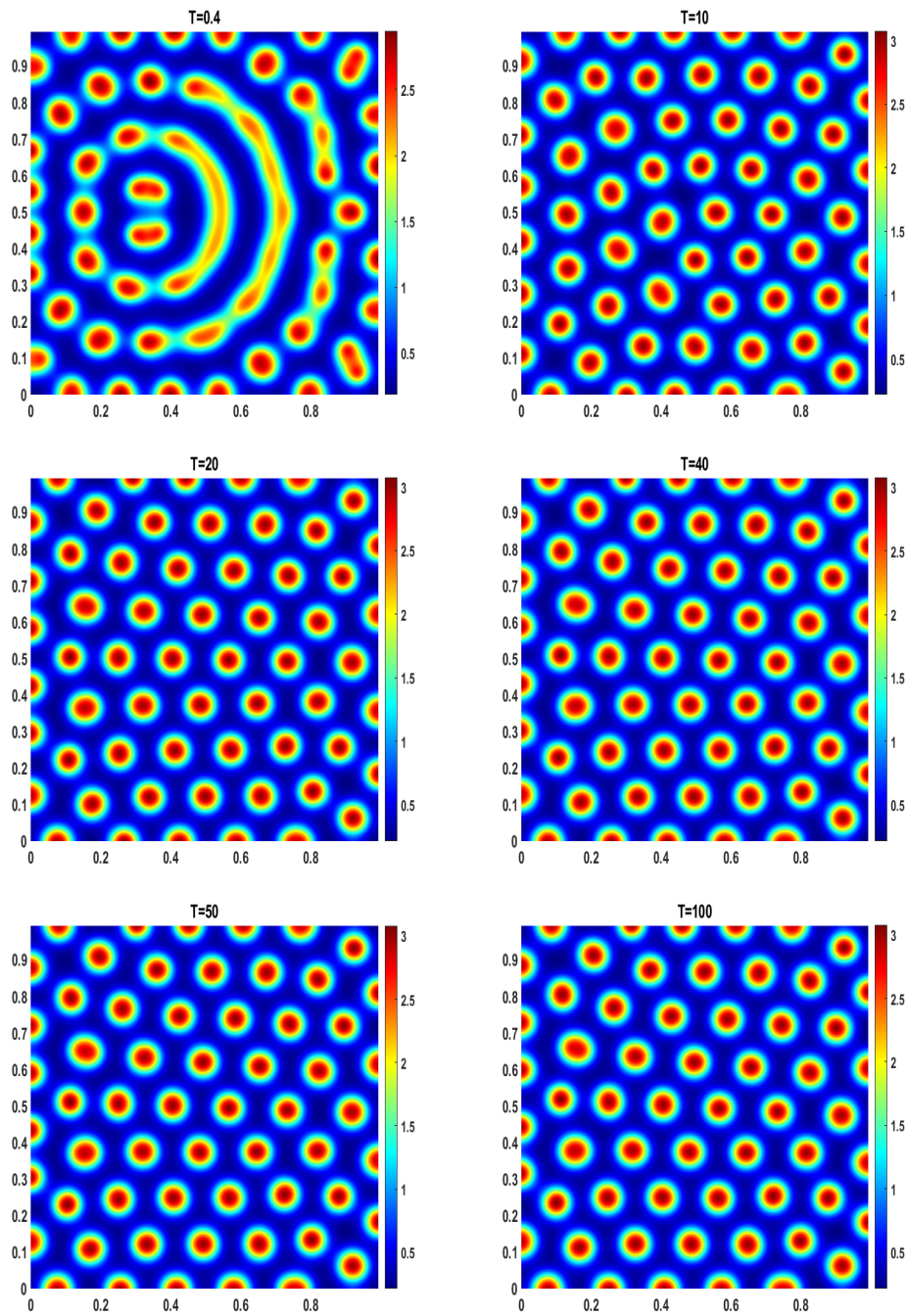


Figure 11: Pattern formation with $\gamma_1 = 230.82$, $\gamma_2 = 0.1$, $\gamma_3 = 0.9$, $\mu_{11} = 0.05$, $\mu_{22} = 1$ and $2\nu = 2\eta = 1.9$.

Table 1: Error obtained based on the reference solution for case 1.

N	Finite difference method	Finite element method	Present method	CPU time(s)
	$\mathcal{E}_{u,\infty}^N$	$\mathcal{E}_{u,\infty}^N$	$\mathcal{E}_{u,\infty}^N$	
100	5.3624×10^{-2}	6.1207×10^{-2}	2.0264×10^{-3}	16
200	7.4102×10^{-3}	8.1011×10^{-3}	5.2135×10^{-4}	48
400	6.7176×10^{-4}	1.3001×10^{-3}	1.3138×10^{-4}	87
800	1.0318×10^{-4}	6.1733×10^{-4}	3.3039×10^{-5}	163
1600	8.6480×10^{-5}	9.6634×10^{-5}	8.3013×10^{-6}	230
3200	2.0034×10^{-5}	4.0001×10^{-5}	2.0775×10^{-7}	374

Table 2: Error obtained based on the reference solution for case 2.

N	Finite difference method	Finite element method	Present method	CPU time(s)
	$\mathcal{E}_{v,\infty}^N$	$\mathcal{E}_{v,\infty}^N$	$\mathcal{E}_{v,\infty}^N$	
100	7.2145×10^{-2}	7.0143×10^{-2}	4.2287×10^{-3}	16
200	8.6410×10^{-3}	7.5540×10^{-3}	7.6482×10^{-4}	48
400	7.1002×10^{-4}	2.0413×10^{-3}	2.0006×10^{-4}	87
800	2.0036×10^{-4}	5.4969×10^{-4}	4.6741×10^{-5}	163
1600	9.4510×10^{-5}	1.2348×10^{-4}	7.4461×10^{-6}	230
3200	3.3317×10^{-5}	6.8977×10^{-5}	6.5543×10^{-7}	374

References

- [1] J. Shin, S-K Park and J. Kim, A hybrid FEM for solving the Allen–Cahn equation, *Appl. Math. Comput.* **244** (2014) 606–612, <https://doi.org/10.1016/j.amc.2014.07.040>.
- [2] A. Gierer and H. Meinhardt, A theory of biological pattern formation, *Kybernetik* **12** (1972) 30–39, <https://doi.org/10.1007/BF00289234>.
- [3] M. Alber, T. Glimm, H. G. E. Hentschel, B. Kazmierczak, Y-T Zhang, J. Zhu, and S. A. Newman, The morphostatic limit for a model of skeletal pattern formation in the vertebrate limb, *Bull. Math. Biol.* **70** (2) (2008) 460–483, <https://doi.org/10.1007/s11538-007-9264-3>.
- [4] I. A. Pavel’chak, A numerical method for determining the localized initial condition in the FitzHugh-Nagumo and Aliev-Panfilov models, *MoscowUniv. Comput. Math. Cybern.* **35** (2011) 105–112, <https://doi.org/10.3103/S0278641911030071>.
- [5] M. W. Yasin, M. S. Iqbal, N. Ahmed, A. Akgül, A. Raza, M. Rafiq and M. B. Riaz, Numerical scheme and stability analysis of stochastic FitzHugh-Nagumo model, *Results Phys.* **32** (2022) p. 105023, <https://doi.org/10.1016/j.rinp.2021.105023>.
- [6] R. Chertovskih, E. L. Rempel and E. V. Chimanski, Magnetic field generation by intermittent convection, *Phys. Lett. A* **381** (38) (2017) 3300–3306, <https://doi.org/10.1016/j.physleta.2017.08.025>.
- [7] M. Dehghan and V. Mohammadi, The boundary knot method for the solution of two-dimensional advection reaction-diffusion and Brusselator equations, *Int. J. Numer. Methods Heat Fluid Flow* **31** (1) (2020) 106–133, <https://doi.org/10.1108/HFF-10-2019-0731>.

- [8] Z. Lin, R. Ruiz-Baier and C. Tian, Finite volume element approximation of an inhomogeneous Brusselator model with cross-diffusion, *J. Comput. Phys.* **256** (2014) 806–823, <https://doi.org/10.1016/j.jcp.2013.09.009>.
- [9] E. H. Twizell, A. B. Gumel and Q. Cao, A second-order scheme for the “Brusselator” reaction–diffusion system, *J. Math. Chem.* **26** (1999) 297–316, <https://doi.org/10.1023/A:1019158500612>.
- [10] M. Dehghan and M. Abbaszadeh, Variational multiscale element free Galerkin (VMEFG) and local discontinuous Galerkin (LDG) methods for solving two-dimensional Brusselator reaction–diffusion system with and without cross-diffusion, *Comput. Methods Appl. Mech. Eng.* **300** (2016) 770–797, <https://doi.org/10.1016/j.cma.2015.11.033>.
- [11] R. Jiwari and J. Yuan, A computational modeling of two dimensional reaction–diffusion Brusselator system arising in chemical processes, *J. Math. Chem.* **52** (2014) 1535–1551, <https://doi.org/10.1007/s10910-014-0333-1>.
- [12] J. D. Murray, *Mathematical Biology II: Spatial Models and Biomedical Applications*, Springer New York, 2003.
- [13] R. C. Sarker and S. K. Sahani, Turing pattern dynamics in an SI epidemic model with superdiffusion, *Internat. J. Bifur. Chaos Appl. Sci. Engrg.* **32** (11) (2022) p. 2230025, <https://doi.org/10.1142/S0218127422300257>.
- [14] R. M. Jena, S. Chakraverty, H. Rezazadeh and D. Domiri Ganji, On the solution of time-fractional dynamical model of Brusselator reaction-diffusion system arising in chemical reactions, *Math. Methods Appl. Sci.* **43** (7) (2020) 3903–3913, <https://doi.org/10.1002/mma.6141>.
- [15] F. Muhammad Khan, A. Ali, K. Shah, A. Khan and I. Mahariq, Analytical approximation of brusselator model via ladm, *Math. Probl. Eng.* **2022** (2022) Article ID 8778805, <https://doi.org/10.1155/2022/8778805>.
- [16] S. Alshammari, M. M. Al-Sawalha and J. R. Humaidi, Fractional view study of the Brusselator reaction–diffusion model occurring in chemical reactions, *Fractal Fract.* **7** (2023) p. 108, <https://doi.org/10.3390/fractalfract7020108>.
- [17] K. M. Saad, Fractal-fractional Brusselator chemical reaction, *Chaos Solit. Fractals* **150** (2021) p. 111087, <https://doi.org/10.1016/j.chaos.2021.111087>.
- [18] M. Izadi and H. M. Srivastava, Fractional clique collocation technique for numerical simulations of fractional-order Brusselator chemical model, *Axioms* **11** (11) (2022) p. 654, <https://doi.org/10.3390/axioms11110654>.
- [19] J. Singh, M. M. Rashidi, D. Kumar and R. Swroop, A fractional model of a dynamical Brusselator reaction-diffusion system arising in triple collision and enzymatic reactions, *Nonlinear Eng.* **5** (4) (2016) 277–285, <https://doi.org/10.1515/nleng-2016-0041>.
- [20] H. Fallahgoul, S. Focardi and F. Fabozzi, *Fractional Calculus and Fractional Processes with Applications to Financial Economics: Theory and Application*, Academic Press, 2016.
- [21] F. Mainardi, Fractional calculus: theory and applications, *Mathematics* **6** (9) (2018) p. 145, <https://doi.org/10.3390/math6090145>.

- [22] I. Podlubny, *Fractional Differential Equations: An Introduction to Fractional Derivatives, Fractional Differential Equations, To Methods of Their Solution and Some of Their Applications*, Elsevier, 1998.
- [23] Z. Jackiewicz, *General Linear Methods for Ordinary Differential Equations*, John Wiley & Sons, 2009.
- [24] J. Li, F. Liu, L. Feng and I. Turner, A novel finite volume method for the Riesz space distributed-order diffusion equation, *Comput. Math. Appl.* **74** (4) (2017) 772–783, <https://doi.org/10.1016/j.camwa.2017.05.017>.
- [25] M. Chen and W. Deng, A second-order accurate numerical method for the space-time tempered fractional diffusion-wave equation, *Appl. Math. Lett.* **68** (2017) 87–93, <https://doi.org/10.1016/j.aml.2016.12.010>.
- [26] A. Mohebbi, Finite difference and spectral collocation methods for the solution of semilinear time fractional convection-reaction-diffusion equations with time delay, *J. Appl. Math. Comput.* **61** (2019) 635–656, <https://doi.org/10.1007/s12190-019-01267-w>.
- [27] A. Saadatmandi and M. Dehghan, A new operational matrix for solving fractional-order differential equations, *Comput. Math. Appl.* **59** (3) (2010) 1326–1336, <https://doi.org/10.1016/j.camwa.2009.07.006>.
- [28] A. Saadatmandi and M. Dehghan, A tau approach for solution of the space fractional diffusion equation, *Comput. Math. Appl.* **62** (3) (2011) 1135–1142, <https://doi.org/10.1016/j.camwa.2011.04.014>.
- [29] M. Pourbabaee and A. Saadatmandi, A new operational matrix based on Müntz–Legendre polynomials for solving distributed order fractional differential equations, *Math. Comput. Simulation* **194** (2022) 210–235, <https://doi.org/10.1016/j.matcom.2021.11.023>.
- [30] M. Dehghan and M. Abbaszadeh, An efficient technique based on finite difference/finite element method for solution of two-dimensional space/multi-time fractional Bloch–Torrey equations, *Appl. Numer. Math.* **131** (2018) 190–206, <https://doi.org/10.1016/j.apnum.2018.04.009>.
- [31] M. R. Ahmadi Darani and A. Saadatmandi, The operational matrix of fractional derivative of the fractional-order Chebyshev functions and its applications, *Comput. Methods Differ. Equ.* **5** (1) (2017) 67–87.
- [32] M. Pourbabaee and A. Saadatmandi, Collocation method based on Chebyshev polynomials for solving distributed order fractional differential equations, *Comput. Methods Differ. Equ.* **9** (3) (2021) 858–873, <https://doi.org/10.22034/CMDE.2020.38506.1695>.
- [33] A. Saadatmandi, A. Khani and M. R. Azizi, Numerical calculation of fractional derivatives for the sinc functions via Legendre polynomials, *Math. Interdisc. Res.* **5** (2) (2020) 71–86, <https://doi.org/10.22052/MIR.2018.96632.1074>.
- [34] M. Abbaszade and A. Mohebbi, Fourth-order numerical solution of a fractional PDE with the nonlinear source term in the electroanalytical chemistry, *Iranian J. Math. Chem.* **3** (2) (2012) 195–220, <https://doi.org/10.22052/IJMC.2012.5147>.
- [35] M. Abbaszadeh, Error estimate of second-order finite difference scheme for solving the Riesz space distributed-order diffusion equation, *Appl. Math. Lett.* **88** (2019) 179–185, <https://doi.org/10.1016/j.aml.2018.08.024>.

- [36] H. Ding, C. Li and Y. Chen, High-order algorithms for Riesz derivative and their applications (ii), *J. Comput. Phys.* **293** (2015) 218–237, <https://doi.org/10.1016/j.jcp.2014.06.007>.
- [37] X. Zhao, Z. Sun and Z. Hao, A fourth-order compact ADI scheme for two-dimensional nonlinear space fractional schrödinger equation, *SIAM J. Sci. Comput.* **36** (6) (2014) A2865–A2886, <https://doi.org/10.1137/140961560>.
- [38] C. Li, Q. Yi and A. Chen, Finite difference methods with non-uniform meshes for nonlinear fractional differential equations, *J. Comput. Phys.* **316** (2016) 614–631, <https://doi.org/10.1016/j.jcp.2016.04.039>.
- [39] A. H. Bhrawy and M. A. Zaky, An improved collocation method for multi-dimensional space–time variable-order fractional schrödinger equations, *Appl. Numer. Math.* **111** (2017) 197–218, <https://doi.org/10.1016/j.apnum.2016.09.009>.
- [40] A. H. Bhrawy, M. A. Zaky and R. A. Van Gorder, A space-time Legendre spectral tau method for the two-sided space-time Caputo fractional diffusion-wave equation, *Numer. Algor.* **71** (1) (2016) 151–180, <https://doi.org/10.1007/s11075-015-9990-9>.
- [41] M. Abbaszadeh and M. Dehghan, An improved meshless method for solving two-dimensional distributed order time-fractional diffusion-wave equation with error estimate, *Numer. Algor.* **75** (2017) 173–211, <https://doi.org/10.1007/s11075-016-0201-0>.
- [42] A. S. Hendy and M. A. Zaky, Graded mesh discretization for coupled system of nonlinear multi-term time-space fractional diffusion equations, *Eng. Comput.* **38** (2022) 1351–1363, <https://doi.org/10.1007/s00366-020-01095-8>.
- [43] A. S. Hendy, M. A. Zaky and J. E. Macías-Díaz, On the dissipativity of some Caputo time-fractional subdiffusion models in multiple dimensions: theoretical and numerical investigations, *J. Comput. Appl. Math.* **400** (2022) p. 113748, <https://doi.org/10.1016/j.cam.2021.113748>.
- [44] M. A. Zaky, A. S. Hendy and D. Suragan, Logarithmic Jacobi collocation method for Caputo–Hadamard fractional differential equations, *Appl. Numer. Math.* **181** (2022) 326–346, <https://doi.org/10.1016/j.apnum.2022.06.013>.
- [45] A. Bhrawy and M. Zaky, A fractional-order Jacobi tau method for a class of time-fractional pdes with variable coefficients, *Math. Methods Appl. Sci.* **39** (7) (2016) 1765–1779, <https://doi.org/10.1002/mma.3600>.
- [46] H. Liao, P. Lyu and S. Vong, Second-order BDF time approximation for Riesz space-fractional diffusion equations, *Int. J. Comput. Math.* **95** (1) (2018) 144–158, <https://doi.org/10.1080/00207160.2017.1366461>.
- [47] M. Hamid, M. Usman, Y. Yan and Z. Tian, An efficient numerical scheme for fractional characterization of MHD fluid model, *Chaos Solitons Fractals* **162** (2022) p. 112475, <https://doi.org/10.1016/j.chaos.2022.112475>.
- [48] M. Abbaszadeh, M. Golmohammadi and M. Dehghan, Simulation of activator–inhibitor dynamics based on cross-diffusion Brusselator reaction–diffusion system via a differential quadrature-radial point interpolation method (DQ-RPIM) technique, *Eur. Phys. J. Plus* **136** (1) (2021) 1–26, <https://doi.org/10.1140/epjp/s13360-020-00872-0>.

- [49] M. Abbaszadeh and M. Dehghan, A reduced order finite difference method for solving space-fractional reaction-diffusion systems: the Gray-Scott model, *Eur. Phys. J. Plus* **134** (2019) 1–15, <https://doi.org/10.1140/epjp/i2019-12951-0>.
- [50] Z. Mao and G. E. Karniadakis, A spectral method (of exponential convergence) for singular solutions of the diffusion equation with general two-sided fractional derivative, *SIAM J. Numer. Anal.* **56** (1) (2018) 24–49, <https://doi.org/10.1137/16M1103622>.
- [51] V. J. Ervin and J. P. Roop, Variational formulation for the stationary fractional advection dispersion equation, *Numer. Methods Partial Differential Equations* **22** (3) (2006) 558–576, <https://doi.org/10.1002/num.20112>.
- [52] W. Bu, Y. Tang, Y. Wu and J. Yang, Finite difference/finite element method for two-dimensional space and time fractional Bloch–Torrey equations, *J. Comput. Phys.* **293** (2015) 264–279, <https://doi.org/10.1016/j.jcp.2014.06.031>.